Potentiating Oncolytic Virus-Induced Immune Mediated Tumor Cell Killing Using Histone Deacetylase Inhibition

Victoria A. Jennings[1,2], Gina B. Scott[2], Ailsa M. S. Rose[2], Karen J. Scott[2], Gemma Migneco[2], Brian Keller[3], Katrina Reilly[2], Oliver Donnelly[2], Howard Peach[4], Donald Dewar[4], Kevin J. Harrington[1], Hardev Pandha[5], Adel Samson[2], Richard G. Vile[6], Alan A. Melcher[1]* and Fiona Errington-Mais[2*].

[1]The Institute of Cancer Research, Division of Radiotherapy and Imaging, Chester Beatty Laboratories, London SW3 6JB, UK.

[2]Section of Infection and Immunity, Leeds Institute of Cancer and Pathology, University of Leeds, Beckett Street, Leeds, LS9 7TF

[3]Ottawa Hospital Research Institute, Ottawa, Canada

[4]St James's University Hospital, Leeds, LS9 7TF

[5]Leggett Building, Faculty of Health and Medical Sciences, University of Surrey, Guildford GU2 7WG, UK.

[6]Mayo Clinic, Rochester, MN 55905, USA.

*Authors contributed equally to this manuscript.

Corresponding Author: Prof Alan Melcher. The Institute of Cancer Research, Division of Radiotherapy and Imaging, Chester Beatty Laboratories, 237 Fulham Road London SW3 6JB, UK. Phone: 02071535205. E-mail: alan.melcher@icr.ac.uk

Running Title: Increasing the therapeutic potential of HSV^{GMCSF}

ABSTRACT

A clinical oncolytic herpes simplex virus (HSV) encoding GM-CSF, talimogene laherparepvec, causes regression of injected and non-injected melanoma lesions in patients and is now licensed for clinical use in advanced melanoma. To date, limited data is available regarding the mechanisms of human anti-tumor immune priming, an improved understanding of which could inform the development of future combination strategies with improved efficacy. This study addressed direct oncolysis and innate/adaptive human immune-mediated effects of a closely related HSV encoding GM-CSF ($HSV^{GM\text{-}CSF}$), alone and in combination with histone deacetylase inhibition. We found that $HSV^{GM\text{-}CSF}$ supported activation of anti-melanoma immunity via monocyte-mediated type I interferon production, which activates NK cells, and viral maturation of immature dendritic cells (iDC) into potent antigen presenting cells for cytotoxic T lymphocyte (CTL) priming. Addition of the histone deacetylase inhibitor, valproic acid (VPA), to $HSV^{GM\text{-}CSF}$ treatment of tumor cells, increased viral replication, viral GMCSF production and oncolysis, and augmented the development of anti-tumor immunity. Mechanistically, VPA increased expression of activatory ligands for NK cell recognition, and induced expression of tumor-associated antigens, thus supporting innate NK cell killing and CTL priming. These data support the clinical combination of talimogene laherparepvec with histone deacetylase inhibition to enhance oncolysis and anti-tumor immunity.

INTRODUCTION

Oncolytic viruses (OVs) are naturally occurring or genetically-engineered viruses with specific anti-tumor effects, mediated both by direct oncolysis and the activation of innate and adaptive anti-tumor immunity. A range of OVs have progressed to clinical studies, and some viruses (e.g. herpes simplex, vaccinia and reovirus) have reached evaluation in randomised clinical trials (1). The most clinically advanced agent (approved for use in the US, Europe and Australasia) is a genetically-modified double-stranded DNA herpes simplex virus (HSV; JS-1 strain) called talimogene laherparepvec (T-Vec). This virus has been rendered tumor selective through functional deletion of ICP34.5; further deletion of ICP47 enhances antigen presentation and brings the viral US11 gene under the control of the ICP47 immediate-early promoter, enhancing tumor-selective replication (2). In addition, the ICP34.5 gene has been replaced with a cassette encoding human GM-CSF to facilitate priming of an anti-tumor immune response (3), and an initial clinical report has confirmed that the virus can convert an immunologically suppressive, 'cold' tumor microenvironment (TME) into an immune-activating 'hot' milieu (4). Hence, T-Vec has a dual mode of action, causing direct tumor cell lysis and bystander activation of an anti-tumor immune response.

Following a phase I study demonstrating acceptable toxicity (5), phase II testing of intratumoral T-Vec, in patients with advanced melanoma, resulted in a 26% response rate with durable responses observed in both injected and uninjected lesions (6). Distant responses suggested generation of anti-tumor immunity, which was consistent with experiments showing an increase in melanoma-associated antigen-specific T cells and a decrease in regulatory/suppressive T cells in tumors after treatment (7). This encouraging clinical trial data led to a randomised phase III

study in melanoma, comparing intratumoral injection against subcutaneous GM-CSF (8), which achieved its primary endpoint of durable response rate (9). Early clinical trials also demonstrated that T-Vec was present in the blood and uninjected lymph nodes, as well as the injected tumor (5,10), suggesting that viral systemic immune activation, and priming instigated within the directly targeted TME, may play an additional role in bystander immune-mediated therapy. Randomised trials, testing combination of T-Vec with immune checkpoint inhibitors in melanoma, have now been completed, with early results showing significant promise (4,11).

Despite this clinical progress, pre-clinical data on the mechanisms responsible for the therapeutic potential of T-Vec is relatively limited, and further information would inform the development of future combination therapies. One promising strategy is to combine OV with histone deacetylase (HDAC) inhibitors (HDACi) which regulate chromatin structure and gene transcription. Histone acetylation is regulated by the opposing actions of histone acetyltransferases (HATs), which mediate the acetylation of histone residues allowing gene transcription, whilst HDACs remove acetyl groups, allowing the negatively charged DNA to bind the nucleosome, acting as transcriptional repressors. HDACs are classified based on their sequence homology and structural similarity providing four different sub classes: class I HDACs (HDAC 1, 2, 3, and 8), class II HDACs (HDAC 4, 5, 7, 9, and 10), class III HDACs (sirtuins), and the class IV HDAC (HDAC11). High expression of class I and II HDACs have been associated with poor patient outcomes and HDACi have been developed as anticancer agents. HDACi induce a diverse range of biological responses in tumors including apoptosis, suppressed proliferation of malignant cells, inhibition of angiogenesis, and immunomodulation (12-15). Specifically, in terms of immunomodulation, HDACi have been reported to: increase antigen presentation

(through modulation of MHC molecules) to increase T cell recognition; increase NK cell activatory ligand expression and NK cell-mediated killing; increase ICAM-1 expression to promote leukocyte infiltration; enhance immunological synapse formation between T cells and antigen presenting cells (APC); and decrease levels of regulatory T cells (Treg)(13).

Clinically, HDACi have gained FDA approval for the treatment of cancer, including vorinostat and FK228 for the treatment of cutaneous T cell lymphoma (CTCL), belinostat for the treatment of peripheral T cell lymphoma (PTCL); and panobinostat, in combination with bortezomib and dexamethasone, for the treatment of multiple myeloma. Whilst most HDACi have been approved for the treatment of hematological malignancies, numerous studies and clinical trials have examined their activity against solid malignancies such as ovarian and breast cancer (14). Valproic acid (VPA) - an anticonvulsant agent and more recently described HDACi with specificity towards class I and class IIa HDACs - has also been reported to display anticancer properties through the induction of cell differentiation, inhibition of cell proliferation and/or altered immunogenicity. VPA acts by directly inhibiting HDACs but also induces proteasomal degradation of HDAC2, therefore exerting its anticancer properties by both transcription-dependent and transcription-independent mechanisms. Currently, VPA is not FDA-approved for the treatment of cancer; however, it has been extensively studied in pre-clinical models, and has reached phase III clinical testing for cervical and ovarian cancer (15). Pivotally, VPA is an approved treatment option for epilepsy, bipolar disorder, and migraine prevention, and has a well-established safety profile derived from decades of clinical use. Moreover, VPA is a cost-effective treatment option by comparison with newer HDAC

inhibitors making the re-purposing of this agent an attractive option for the treatment of cancer (15).

HDACi, including VPA, have been successfully tested in combination with OVs (16,17) and a range of synergistic mechanisms have been identified, including: i) suppression of anti-viral IFN-responsive gene transcription, leading to increased viral replication, spread and oncolysis/apoptosis; ii) induction of nuclear factor kappa B (NF-κB) signaling, resulting in NF-κB-dependent autophagy; iii) increased viral entry receptor expression and viral entry; iv) abrogation of innate immune-mediated viral clearance; and v) enhancement of adaptive anti-tumor immune responses through enhanced CD8 T cell and macrophage infiltration, and decreased Tregs, with appropriate combination scheduling (18-20). To date, VPA has been reported to enhance HSV and parvovirus replication in cancer cells (21,22) but its efficacy in combination with HSV for melanoma has not been described; moreover, the effect of VPA in OV-induced human immunotherapy remains unknown. Here, we describe the use of clinically relevant human models (23-27) to explore oncolytic $HSV^{GM\text{-}CSF}$ and VPA immune co-operation to support the development of anti-tumor immune responses against human melanoma.

RESULTS

HSV^{GM-CSF} induces innate and adaptive anti-tumor immunity

We have previously developed *in vitro*, pre-clinical assays, to test the potential of OVs to support the activation of human innate (dendritic cells (DC) and natural killer (NK) cells) and adaptive (cytotoxic T lymphocytes; CTL) anti-tumor immunity (23,26-28). To initially address the immunogenicity of HSV^{GM-CSF}, we pulsed the virus onto peripheral blood mononuclear cells (PBMC) taken from healthy donors and melanoma patients and examined activation of NK cells. Addition of HSV^{GM-CSF} induced NK cell degranulation (the release of cytotoxic granules) in both healthy donors (Fig 1A) and patient samples (Fig 1B) upon co-culture with melanoma cell targets, as determined by increased expression of CD107 on NK cells. Importantly, HSV^{GM-CSF}-induced NK cell degranulation correlated with increased lysis of melanoma cell targets (Fig 1C). To confirm that NK cells were responsible for melanoma target cell death, in the context of PBMC, we have shown that: i) depletion of NK cells from PBMC significantly reduced killing of MEL888 cells (Supplementary Fig S1A); and ii) that killing was mediated by perforin/granzyme (pivotal components of NK cell cytotoxic granules), as cell lysis was abrogated by EGTA, a calcium chelator that prevents the activity of calcium-dependent perforin (Supplementary Fig S1B).

Having previously shown that OV can activate DC, pivotal APCs that bridge both the innate and adaptive arms of the immune system (23), we investigated the effect of HSV^{GM-CSF} on DC antigen presenting machinery (MHC class I and II) and co-stimulatory molecules (CD80 and CD86). We found that HSV^{GM-CSF} induced

maturation of immature DC (iDC), causing a significant upregulation of CD80 and CD86, and retention of MHC class I and II (Fig 1D) without significantly decreasing cell viability (data not shown). Next, to determine whether iDC were infected with $HSV^{GM\text{-}CSF}$, and if this was required to induce DC maturation, we treated iDC with GFP-expressing HSV (0.01 and 0.1pfu/cell) and examined CD86 expression in GFP-positive (HSV-infected) and GFP-negative (non-infected) DC. At the highest MOI, approximately 10% of DC were GFP-positive, and in accordance with this a 10% loss in viability was observed, demonstrating that DC were indeed permissive to HSV-infection and subsequent cell death (data not shown). However, importantly, CD86 up-regulation was observed in GFP-negative DC suggesting an indirect mechanism of DC maturation, potentially mediated by cytokine release (data not shown).

Furthermore, co-culture of $HSV^{GM\text{-}CSF}$-infected tumor cells with iDC resulted in increased secretion of GM-CSF and TNFα, together with decreased production of the immunosuppressive cytokine, IL-10 (Fig 1E); virus-infected melanoma cells secrete GM-CSF, as expected (Fig 3), therefore it is most likely that the GM-CSF production is derived from infected tumor cells; however, given that up to 10% of DC can be infected by HSV it is also possible that DC may contribute to GMCSF production. Moreover, MEL888 cells secrete IL-10, which can be down-regulated by OV treatment (29), and iDC produce TNFα following OV treatment (30), therefore, whilst we have not specifically demonstrated that the changes in IL-10 and TNFα levels are due to effects on MEL888 cells and iDC, respectively, we postulate that this is the most likely explanation.

Finally, to assess whether $HSV^{GM\text{-}CSF}$-induced DC maturation and changes in the pro-inflammatory cytokine milieu supported adaptive CTL immune priming, we

loaded iDC with $HSV^{GM\text{-}CSF}$-infected tumor cells and examined whether tumor-loaded DC could support the generation of tumor-specific CTL (23,27,28). Figure 1F shows that virus-infected tumor cells supported the generation of melanoma-specific CTL, whilst non-infected tumor cells did not (Fig 1F). Taken together, these data show that $HSV^{GM\text{-}CSF}$ has the potential to enhance both innate and adaptive anti-tumor immune responses.

Activation of a human innate immune response by $HSV^{GM\text{-}CSF}$ is dependent on virus-induced type I interferon production

To characterize the mechanisms responsible for innate NK cell activation following $HSV^{GM\text{-}CSF}$ treatment we first examined the ability of $HSV^{GM\text{-}CSF}$ to activate isolated NK cells. NK cells isolated from PBMC, and subsequently treated with $HSV^{GM\text{-}CSF}$ directly, were unable to degranulate against melanoma targets and showed no upregulation of the early activation marker, CD69 (Fig 2A). Furthermore, when PBMC were depleted of $CD14^+$ monocytes (previously shown to be central to the immune response induced by an alternative OV, reovirus (28)) we found that $HSV^{GM\text{-}CSF}$ treatment did not result in activation of NK cells, as assessed by surface CD69 expression, relative to PBMC which included monocytes (Supplementary Fig S2A); additionally, NK cell-mediated killing was also significantly abrogated (Supplementary Fig S2B). Therefore, these data support a role for monocytes within PBMC in mediating the activation of NK cells by $HSV^{GM\text{-}CSF}$.

Upon further examination, we demonstrated that PBMC treated with $HSV^{GM\text{-}CSF}$ secreted type I, II and III IFNs (Fig 2B) and that blockade of type I IFNα/β abrogated $HSV^{GM\text{-}CSF}$-induced activation of NK cells, in terms of CD69 expression (Fig 2Ci), NK cell CD107 degranulation (Fig 2Cii), and cytotoxicity against melanoma cells (Fig

Ciii). Furthermore, type I IFN production, like NK cell activation, was significantly abrogated when $CD14^+$ monocytes were depleted from PBMC (Fig 2D). Taken together, these data show that the innate response of NK cells following $HSV^{GM\text{-}CSF}$ treatment of PBMC was dependent on type I IFN production, and confirmed a role for $CD14^+$ monocytes in mediating type I IFN secretion.

HDACi enhances $HSV^{GM\text{-}CSF}$ replication, killing and GM-CSF production in melanoma cells

Having shown that $HSV^{GM\text{-}CSF}$ induces innate and adaptive immune responses in our human model systems we subsequently examined the ability of HDACi to potentiate $HSV^{GM\text{-}CSF}$ efficacy in terms of direct cytotoxicity and $HSV^{GM\text{-}CSF}$-induced anti-tumor immunity. First, to investigate the direct cytopathic effects of $HSV^{GM\text{-}CSF}$ in the presence or absence of HDACi, MEL888 cells were pre-treated with a range of HDACi (VPA, tubastatin, vorinostat, droxinostat, givinostat and mocetinostat) for 24hrs before the addition of $HSV^{GM\text{-}CSF}$ (at concentrations up to 2.5 pfu/cell) for a further 48hrs, and cell viability was determined by MTT (Supplementary Fig S3). These data demonstrated that all the HDACi tested were able to enhance $HSV^{GM\text{-}CSF}$ cytotoxicity, although, as expected, the results were variable and greatest potentiation was observed for VPA, givinostat and mocetinostat. Given the long-standing safety profile of VPA, and the cost effective nature of this agent, VPA was selected for further experimentation.

Initially, the ability of VPA to potentiate $HSV^{GM\text{-}CSF}$ cytotoxicity against a larger panel of melanoma cell lines was examined; all cells lines were susceptible to $HSV^{GM\text{-}CSF}$-induced cytotoxicity, with variable sensitivity, and VPA significantly increased the direct cytotoxic effect of $HSV^{GM\text{-}CSF}$ in all cell lines tested (Fig 3A,

Supplementary Fig S4A). Next, the ability of $HSV^{GM\text{-}CSF}$ to induce secretion of GM-CSF and replicate in melanoma cells was determined. GM-CSF was produced upon infection of all cell lines (Fig 3B, Supplementary Fig S4B), although levels were lower in A375 cells compared to MEL888 (Fig 3A); significantly, VPA increased GM-CSF secretion in both the relatively resistant (A375) and sensitive (MEL888) cell lines (Fig 3B). Additionally, plaque assays confirmed the production of infectious progeny virus, and showed that VPA increased $HSV^{GM\text{-}CSF}$ replication (Fig 3C), with potentiation by VPA being most evident in the A375 cells that were inherently less permissive to viral replication. In terms of scheduling of the two reagents, and consistent with previous data (16), we also found that enhanced $HSV^{GM\text{-}CSF}$ replication was dependent on pre-treatment with VPA, otherwise no increase in viral replication was seen (Fig 3C). Importantly, $HSV^{GM\text{-}CSF}$ cytotoxicity against non-neoplastic human foreskin fibroblasts (HFF) was not enhanced upon combination with VPA (Supplementary Fig S5), suggesting that VPA would not increase off-target side effects caused by viraemia in non-malignant tissue. Collectively, these data confirm that $HSV^{GM\text{-}CSF}$ directly infects, kills and replicates in human melanoma cells, resulting in secretion of GM-CSF, and that the addition of VPA potentiates these effects, particularly in cells which are otherwise relatively poorly permissive.

HDACi augments $HSV^{GM\text{-}CSF}$-induced innate anti-tumor immunity

Having shown that VPA increases killing, replication and GM-CSF production upon $HSV^{GM\text{-}CSF}$ treatment of human melanoma cells, we next tested the effects of VPA on $HSV^{GM\text{-}CSF}$-induced innate anti-tumor immunity. To address this, we first tested whether VPA affected the expression of activatory NK ligands on human melanoma cells; VPA has previously been reported to up-regulate NK ligand expression on

acute myeloid leukemia cells, *in vivo* (31,32). We observed an upregulation of the NKG2D ligands, MICA/B, on MEL888 cells, and MICA/B and ULBP-2/5/6 on less permissive A375 cells, upon treatment with VPA (Fig 4A); similar results were also observed using primary melanoma cells (Supplementary Fig S6A, and data not shown). This suggested that the addition of VPA could directly support innate anti-tumor immunity by increasing activatory NK cell:tumor target interactions; this was subsequently confirmed as VPA treatment of melanoma cells, prior to their co-culture with $HSV^{GM\text{-}CSF}$-treated PBMC, caused increased NK cell-mediated tumor cell killing (Fig 4B). Importantly, additional studies have confirmed that alternative HDACi also up-regulate the expression of NK cell activatory ligands on melanoma tumor cells (Supplementary Fig 6B), suggesting that the effects of VPA were due to HDAC inhibition and not an alternative, HDAC-independent, mechanism of action.

Furthermore, in line with previously published data which showed that VPA was only toxic to NK cells at doses greater than 2.5mM (33), we confirmed that pre-treatment of PBMC with VPA prior to $HSV^{GM\text{-}CSF}$ stimulation (e.g. the schedule required for enhanced direct oncolysis) does not inhibit the production of type I IFNα from PBMC (Supplementary Fig S7A), which is necessary for NK cell activation, and accordingly pre-treatment with VPA does not abrogate NK cell CD107 degranulation against melanoma targets (Supplementary Fig S7B). Collectively, these data demonstrate that virus-activated NK cell effector function, combined with HDACi-induced upregulation of NK cell activatory ligands, could be used to potentiate the early, innate phase of OV-mediated anti-tumor immunity.

HDACi enhances $HSV^{GM\text{-}CSF}$-mediated CTL priming against human melanoma.

Having shown that $HSV^{GM\text{-}CSF}$-treated melanoma cells can be used as an 'antigen load' for iDC to prime the generation of CTL (Fig 1F), we went on to examine the consequences of HDAC inhibition for CTL priming. Moreover, to allow more complete characterisation of the CTL response, we developed an immune readout component to allow tracking of T cell responses against a range of tumor-associated antigens (TAA), without HLA restriction. This adaptive immune readout involved pulsing autologous monocytes (capable of antigen processing and presentation) with 15mer overlapping peptides of TAA (melanocyte protein PMEL, PMEL; tyrosinase, TYR; and melanoma antigen recognized by T-cells 1, MART-1/MELAN-A) and co-culturing these with CTL. TAA peptide recall responses by CTL were then analysed by flow cytometry to quantify intracellular IFN-γ production. As shown in Fig 5A, $HSV^{GM\text{-}CSF}$ infection of MEL888 cells enhanced the CD8 response against the MEL888-expressed TAA, PMEL, MART-1 and TYR, with a significant enhancement observed for MART-1 ($p=0.0028$). Moreover, the quantity of TAA-specific responses measured against PMEL and TYR was significantly increased by co-treatment of MEL888 cells with 2mM VPA and $HSV^{GM\text{-}CSF}$ virus, compared to $HSV^{GM\text{-}CSF}$ alone. Interestingly, MEL888 cells treated with 2mM VPA prior to HSV infection then co-cultured with iDC, had significantly reduced levels of IL-10 in cell culture supernatants compared to virus alone controls (Fig 5B), and higher concentrations of IFNγ were detected in CTL culture supernatants (Fig 5C); thus, the cytokine changes resulting from combination treatment may favor the generation of TAA-specific CTL.

As well as addressing whether VPA could boost the CD8 response against TAA which were expressed by melanoma cells, we also considered whether HDACi might alter the expression TAA by melanoma cells, and potentially broaden the range of

antigens available for CTL priming. Initial studies demonstrated that VPA treatment of MEL888 cells did not increase PMEL, MART-1 or TYR expression at the protein level (data not shown). A375 cells do not express PMEL under normal growth conditions; however, following treatment with VPA, or alternative HDACi, significant increases in PMEL mRNA expression levels were detected (Fig 5D and Supplementary Fig S8) Moreover, using flow cytometry and immunofluorescence techniques, we could detect PMEL protein expression following VPA/HSV$^{GM\text{-}CSF}$ co-treatment, but interestingly not following either treatment alone (Fig 5Ei and ii, respectively). Following these observations, the ability of VPA to facilitate the generation of PMEL-specific CTL, using A375 cells as the antigen load, was investigated. Fig 5F shows that only A375 cells treated with VPA/HSV$^{GM\text{-}CSF}$, but not virus alone, were capable of generating PMEL-specific CTL. Taken together, we have shown that HSV$^{GM\text{-}CSF}$ infection supports human adaptive CTL priming against a range of melanoma-associated TAA, and that this priming is further increased by VPA, which can boost both the range and level of responses against targeted epitopes.

DISCUSSION

Oncolytic viruses represent a promising class of novel cytotoxic and immunogenic cancer therapy. Although T-Vec is the most clinically advanced agent, there is little pre-clinical data to inform its future development and optimal use, particularly in human systems. Despite its current application as an intratumoral treatment for melanoma, initial melanoma studies were restricted to testing of a single cell line for cytotoxicity *in vitro* only, using an early form of the virus which did not encode GM-CSF (34). In the current study, we therefore sought to address the role of both direct oncolysis and anti-tumor immunity (both innate and adaptive) in T-Vec efficacy, using a closely related JS-1 strain of HSV-1 virus encoding GM-CSF, both alone and in combination with HDAC inhibition.

In our first experiments, we extended our previous studies using the dsRNA OV reovirus (23,26-28), to test the potential of the DNA virus $HSV^{GM\text{-}CSF}$ to stimulate innate and adaptive anti-melanoma immunity (Fig 1). We found that: i) addition of $HSV^{GM\text{-}CSF}$ to human PBMC activated perforin/granzyme-mediated NK killing of melanoma targets; ii) $HSV^{GM\text{-}CSF}$-induced maturation of iDC, and iii) $HSV^{GM\text{-}CSF}$ infection supported the generation of melanoma-specific CTL. This ability of $HSV^{GM\text{-}CSF}$ to activate innate, and subsequent adaptive anti-tumor immunity, supports its designation as an immunotherapeutic agent in humans. At present, the

consequences of innate immune activation following administration of OV remain controversial. For example, murine models suggest that innate anti-viral NK cell response limits therapy by restricting direct tumor oncolysis (20,33,35,36), by restricting viral replication and spread. Alternatively, NK cells have been shown to be essential for the success of a number of OVs across a range of pre-clinical models (37-41), suggesting the innate response to the virus is critical for therapy. Furthermore, for other HSV, experimental models have demonstrated the dependence of intratumoral HSV-1-induced melanoma therapy on NK cells (42), and studies have described the effectiveness of UV-inactivated HSV in the stimulation of PBMC to kill acute myeloid leukemia tumor cells in the absence of direct oncolysis (43). These lines of evidence support a positive role for the innate response in HSV therapy.

Currently, the clinical use of T-Vec is restricted to intratumoral delivery; however, we know that the virus is subsequently released systemically as it can be detected in the circulation and within lymph nodes (5,10). This viraemia, which is consistent with transient flu-like symptoms and the induction of an anti-viral antibody response, means the virus has the potential to activate anti-tumor immunity systemically, as well as locally within the tumor. Therefore, our study of the human innate effects of $HSV^{GM\text{-}CSF}$ on PBMC, as well as on infected melanoma cells as the antigen load in a CTL priming assay, remains clinically relevant. However, it is also important to note that HSV will initially engage an immunologically suppressive TME comprising Tregs, myeloid derived suppressor cells (MDSC) and M2-polarised macrophages; however, despite this, HSV has the capacity to modulate the TME (4) to enrich levels of melanoma-specific effector T cells, and decrease levels of Treg at the site of tumor viral injection (7). Interestingly, HSV has been reported to inactivate MDSC (44) and

it is possible that HSV injection could increase NK cell infiltration at the tumor site, as described for alternative OVs (45), but remains undescribed for T-vec.

The work illustrated is especially important as the effects described here cannot be reliably modelled in murine systems. In particular, we tried testing of $HSV^{GM\text{-}CSF}$ alone, or in combination with VPA, in murine *in vitro* and *in vivo* systems, but found that mouse tumor cells (e.g. B16 melanoma) were far more resistant to $HSV^{GM\text{-}CSF}$ than human melanoma cells, and VPA was unable to increase NK cell activatory ligands on murine melanoma cells. However, despite no meaningful comparative results being obtained in murine models, we believe this was due to major inherent differences between human melanoma models and murine immunocompetent models (in particular, only humans are the natural hosts for type I HSV) rather than any lack of potential combination therapeutic benefit to patients.

In terms of the mechanisms by which HSV activates a human immune response we found, as with reovirus (25), that the production of type I interferons, mediated by monocytes, was required (Fig 2). However, these innate responses are not identical for all OVs; for example, monocytes are not required for IFN production induced by ssRNA coxsackievirus (unpublished data), and the IFN-γ and IL-29 secretion we observed in response to $HSV^{GM\text{-}CSF}$ (Fig 2C), was not seen with reovirus (23,46). The detailed mechanisms by which viral detector cells respond to ssRNA, dsRNA and DNA viruses, and how these shape the ensuing adaptive immune response, are worthy of further study, and are likely to inform the development of optimally immunogenic virotherapy, particularly as part of combination strategies. However, despite the clear role for monocytes in type I IFN production and subsequent NK cell activation, NK cells were still activated (albeit to a lesser extent) in the absence of monocytes, and low level IFNα production was still observed. Therefore, it is

possible that alternative mechanisms may also be involved in the detection of HSV; for example, plasmacytoid DC have also been reported to play a role in regulating anti-HSV immune responses (47-49).

Amongst the various immunomodulatory strategies to have been tested in combination with OV, HDACi have been explored as a means to enhance virus-mediated oncolysis, via suppression of the tumor cells anti-viral IFN response, following infection (16,33). However, HDAC inhibition has a wide range of consequences, and a recent study demonstrated, using cDNA arrays, that the expression of 10–20% of genes were altered following treatment with HDACi (50). We found that pre-treatment of human melanoma cell lines with VPA increased cytotoxicity, GM-CSF secretion and viral replication upon infection with $HSV^{GM\text{-}CSF}$ (Fig 3), although no effect of HDACi on IFN production, or the expression of interferon-stimulated genes, by tumor cells was observed following virus infection (data not shown). In fact, we were unable to detect IFNα, IFNβ, IL-28a or IL28b/IL-29 by ELISA following $HSV^{GM\text{-}CSF}$ and gene expression results confirmed that viral treatment did not induce an IFN signalling cascade (data not shown). Moreover, we also explored the possibility that VPA could alter the surface expression of HSV receptors, HVEM and Nectin 1, or alter NFkB signalling (51); no changes were observed following VPA treatment (data not shown). Currently the mechanisms responsible for enhanced $HSV^{GM\text{-}}$CSF-induced direct oncolysis following VPA treatment remain to be fully elucidated; however, an alternative mechanism could be that VPA alteration of chromatin structure prevents $HSV^{GM\text{-}CSF}$ from “hiding” within DNA, thus making it more accessible for viral replication (52).

Perhaps more importantly, from an immune perspective we found that HDACi upregulated expression of NKG2D ligands on melanoma cells, leading to increased

NK cell killing by $HSV^{GM\text{-}CSF}$-activated PBMC (Fig 4). Furthermore, in a novel assay, which quantified non-HLA-restricted anti-TAA CTL priming, the addition of HDACi to $HSV^{GM\text{-}CSF}$ treatment of melanoma cells enhanced both the magnitude and range of TAA expressed by tumor cells as targets for CD8 T-cell recognition (Fig 5). While it was unexpected that PMEL expression was only observed at the protein level upon co-treatment of VPA and $HSV^{GM\text{-}CSF}$, since HSV infection is usually associated with "shut-off" of host protein translation to limit viral detection and allow propagation (53,54), the balance between histone acetylation/deacetylation is important for HSV propagation (55). Therefore, it is possible that HDAC inhibition by VPA allows transcription of PMEL mRNA for subsequent processing in HSV-infected cells, where HSV will employ a range of strategies to stimulate viral protein synthesis, including enhancement of translation initiation and prevention of translation shutdown following cell stress (54). We are currently investigating whether the expanded range of antigens recognised by primed CTL on combination HDACi/$HSV^{GM\text{-}CSF}$ treatment extends to neoantigens as well as the shared, non-mutated TAA, that we have tracked here, and whether this is reflected in the T cell receptor repertoire which develops over time. Importantly, in terms of clinical application of VPA with $HSV^{GM\text{-}CSF}$, the doses of VPA used to potentiate direct oncolysis and anti-tumor immunity would be clinically achievable with current therapeutic ranges for epilepsy and mania ranging between 20-125mg/L (0.15-0.87mM), only marginally lower than the doses utilized in this study; higher serum concentration are clinically achievable with appropriate monitoring of additional toxicities (56,57).

In summary, we have shown, using clinically relevant human pre-clinical models of innate and adaptive anti-tumor immune priming, that $HSV^{GM\text{-}CSF}$ is capable of activating an anti-melanoma immune response, and that the cytotoxicity and

replication, as well as immunogenicity, of the currently most clinically advanced class of OV, is further boosted by combination treatment with HDAC inhibition. This data provides a platform to explore further OV/immunotherapy combination strategies in human pre-clinical systems, and supports the incorporation of clinical HDACi into future HSV-based OV clinical trials.

MATERIALS AND METHODS

Cell culture and reagents

A375, MeWo and Vero cell lines were purchased from ATCC and authenticated using STR profiling and comparison with the DSMZ database. MEL888 (58), and MM96 (59) were obtained from the Cancer Research UK cell bank and MCF-7 were kindly provided by M Muthana (Department of Oncology and Metabolism, University of Sheffield). In the absence of a reference profile within the DSMZ database, cell lines were shown to have an original STR profile which was distinct from all other cell lines within the database. HFF were also purchased from ATCC. All cell lines, and HFFs, were grown in glutamine-containing DMEM (Sigma-Aldrich Ltd), supplemented with 10% FCS (*v*/*v*) (Biosera). All cell lines were routinely checked for mycoplasma and were free from contamination.

PBMC were isolated from healthy donor volunteers or melanoma patients after written, informed consent was obtained in accordance with local institutional ethics and review approval (06/Q1206/106). PBMC were isolated from whole blood by density gradient centrifugation on Lymphoprep (Aldere) and cultured at $2x10^6$cells/ml in glutamine-containing RPMI (Sigma-Aldrich Ltd), supplemented with 10% FCS (*v*/*v*). Where indicated, NK cells were freshly isolated, or $CD14^+$ cells removed/isolated from PBMC using MACS isolation procedures, following the manufacturer's protocols (Miltenyi Biotec). Immature DC (iDC) were generated by culturing CD14+ cells in glutamine-containing RPMI supplemented with 10% FCS (*v/v*), recombinant human IL-4 500 IU/ml and GM-CSF 800 IU/ml (both R&D systems) at a cell density of 1-2 x10^6 cells/ml for 5 days. Cytotoxic T lymphocytes (CTL) were cultured at 4x10^6 cells/ml in glutamine-containing RPMI supplemented

with 7.5% (*v/v*) human AB serum, 1 mM sodium pyruvate, 1 mM HEPES; 1% (*v/v*) non-essential amino acids, 20 μM 2β-mercaptoethanol (all Sigma-Aldrich Ltd) and recombinant human IL-7 (5 ng/ml) (Miltenyi Biotec). Valproic acid (VPA) (Sigma-Aldrich Ltd) was added to cell cultures at 0,1 or 2 mM for indicated durations.

Viruses

JS1 34.5-hGM-CSF 47-pA+ ($HSV^{GM\text{-}CSF}$) was kindly provided by Amgen and virus titre determined by standard plaque assay on Vero cells. The JS1 34.5-hGM-CSF 47-pA+ used in these studies differs from the clinical agent, tamilogene laherparepvec, in that the US11 gene is not under the control of the ICP47 intermediate-early promoter, due to the addition of a poly-A sequence between the promotor and US11 coding sequence.

$HSV^{GM\text{-}CSF}$ replication

Cells were treated with $HSV^{GM\text{-}CSF}$ alone, $HSV^{GM\text{-}CSF}$ following 24hr pre-treatment with VPA or $HSV^{GM\text{-}CSF}$/VPA simultaneously. Cells and supernatants were harvested and subjected to three rounds of freeze/thaw using a 37°C water bath and methanol/dry ice. $HSV^{GM\text{-}CSF}$ concentration was determined by standard plaque assay on Vero cells and fold increase in virus titre was determined by comparison with input virus.

MTT Cell Viability

Melanoma cell lines were seeded at $8x10^3$ cell/well into 96-well plates and left to adhere overnight. Cells were treated with $HSV^{GM\text{-}CSF}$ at indicated doses for 48 hrs (± pre-treatment with VPA for 24 hrs). 20μl MTT (5mg/ml; Sigma-Aldrich Ltd) was

added to cells 4 hrs prior to the end of the incubation period before tissue culture supernatant was removed and cells were solubilised using 150µL DMSO (Sigma-Aldrich Ltd). Optical density absorbance readings were determined using a Thermo Multiskan EX plate reader (Thermo Fisher Scientific), at 540 nm absorbance.

ELISA

The production of human GM-CSF, IFNα (both Mabtech), IFNβ (PBL Interferon Source), IL-10, TNFα IFNγ (all BD Pharmingen) and IL-29, (R & D Systems) in cell free supernatant was determined using matched-paired antibodies according to the manufacturers' instructions. Optical density absorbance readings were determined using a Thermo Multiskan EX plate reader (Thermo Fisher Scientific), at 405 nm absorbance.

Cell Surface Phenotyping

Cell surface expression of indicated markers were quantified by flow cytometry. Briefly, cells were harvested, washed in FACS buffer (PBS; 1% (*v/v*) FCS; 0.1% (*w/v*) sodium azide), incubated for 30 mins at 4˚C with specific antibodies or matching isotype controls. Cells were washed with FACS buffer and then fixed with 1% PFA (1% (*w/v*) paraformaldhyde in PBS) and stored at 4˚C prior to acquisition. Flow cytometry analysis was performed either using a FACSCaliber (and analysis carried out using Cell Quest Pro software (BD Biosciences), an Attune flow cytometer (Life Technologies, with analysis performed on its accompanying software) or a CytoFLEX S (Beckman Coulter) and analysis carried out using CytExpert software.

Intra-Cellular Staining

Cells were cell-surfaced stained and fixed overnight with 1% PFA prior to permeabilisation with 0.3% Saponin (Sigma-Aldrich Ltd) for 15mins at 4˚C. Cells were washed with 0.1% Saponin, incubated with specific antibodies or matched isotype controls for 30 mins at 4˚C. If the primary antibody was fluorescently-unconjugated, cells were then incubated with a matched fluorescently-conjugated antibody for 30 mins a 4˚C. Cells were washed with PBS and flow cytometry analysis was performed immediately using a CytoFLEX S.

Flow Cytometry Antibodies

CD11c APC-Vio770 (MJ4-27G12, Miltenyi Biotec), CD14-PerCP (TUK4, Miltenyi Biotec) CD86-PE-Cy7 (2331, BD biosciences), CD80-PE (L307.4, BD biosciences) HLA-ABC-VioBlue (REA230, Miltenyi Biotec), HLA-DR/DP/DQ-FITC (Tu39, BD biosciences), CD3-PerCP (SK7, BD biosciences), CD56-PE (B159, BD biosciences), CD8-APC (RPA-T8, BD biosciences) CD107a-FITC (H4A3, BD biosciences), CD107b-FITC (H4B4, BD biosciences), CD69-FITC (FN50, BD biosciences), MICA/B-PE (6D4, BD Biosciences), ULBP2/5/6 (FAB1298p, R&D Systems), IFNγ-BV421 (4S.B3, BD biosciences). Mouse IgG1, κ Isotype Control (PE/FITC/PerCP/PE-Cy7/APC) (MOPC-21, BD biosciences), Mouse IgG2a, κ Isotype Control (FITC/PE) (G155-178, BD biosciences) and REA Control-VioBlue (REA293, Miltenyi Biotec).

CD107a/b NK cell degranulation assay

Healthy donor or melanoma patient PBMC were treated with $HSV^{GM\text{-}CSF}$ overnight and co-cultured with melanoma cell targets at a 10:1 ratio for 1 hour at 37˚C. 10

µg/mL Brefeldin A (BioLegend), anti-CD107a/b, anti-CD3 and anti-CD56 were added for a further 4 hrs at 37˚C before cells were washed with FACS buffer and fixed using 1% PFA. Flow cytometry analysis was performed using either the Attune or CytoFLEX S flow cytometers.

Flow Cytometry Killing Assay

Healthy donor PBMC were activated with $HSV^{GM\text{-}CSF}$ overnight at the indicated concentrations and their ability to kill melanoma cell targets (± VPA/ $HSV^{GM\text{-}CSF}$ pre-treatment) stained with cell tracker green (Molecular Probes) was determined using a standard 5 hr co-culture. Co-cultures were washed and stained for viability using Live/dead fixable dead cell stain (Thermo Fisher Scientific) before analysis using an Attune flow cytometer.

Neutralisation of type I IFNs

PBMC were treated with $HSV^{GM\text{-}CSF}$ overnight in the presence or absence of neutralising antibodies (IFN Block; PBL Interferon Source) or isotype control (IFN Isotype; R & D Systems). IFN block consisted of sheep polyclonal anti-human IFN-α, sheep polyclonal anti-human IFN-β (both used at 1.5%) and mouse monoclonal anti-human IFN-α/β receptor chain 2 (used at 2.5%), as previously described (23). Isotype control consisted of sheep serum (Sigma Aldrich Ltd) used at 3% and mouse IgG2a used at 2.5%. PBMC were then washed and used in CD107 degranulation assays, ^{51}Cr cytotoxicity assays or stained for cell-surface expression of CD69, as described above.

Quantitative real time PCR (qRT-PCR)

Total RNA from cells was isolated using TRiZol (Invitogen™) and 1ug of RNA was used to synthesise cDNA using Maxima Reverse Transcriptase (Thermo Fisher Scientific) according to the manufacturer's instructions. qRT-PCR was carried out with SYBR green mix (Applied Biosciences) using a QuantStudio5 Real-time PCR system (Thermo Fisher Scientific). Primer sequences were: PMEL-F: 5'-TATCATGCCTGTGCCTGGGA-3', PMEL-R:5'- GGGGTACGGAGAAGTCTTGC-3' for PMEL, and EIFα-F: 5'-GATTACAGGGACATCTCAAGGCG-3', EIFα-R 5'-TATCTCTTCTGGCTGTAGGGTGG-3') for the EIFα housekeeping control.

Immunofluorescence

Cells were fixed with 4% PFA and permeabilised with 0.1% Triton X-100 (Sigma-Aldrich Ltd). Samples were incubated with anti-melanoma PMEL antibody (gp100) at a dilution of 1/250 (EP4863 (2)) (Abcam), followed by goat anti-rabbit IgG (Alexa Fluor ® 488) (Abcam) secondary antibody, following manufacturer's instructions. Cells were then imaged using EVOS imaging system (ThermoFisher Scientific).

Cytotoxic T cell priming assay

Melanoma cells were treated ±VPA 24 hrs prior to the addition of $HSV^{GM\text{-}CSF}$ and iDC. Non-adherent cells (iDC loaded with TAA) were removed 24 hrs after the addition of $HSV^{GM\text{-}CSF}$ and cultured with autologous PBMC for 7 days. CTL were re-stimulated (as previously) and cultured for a further 7 days. Primed CTL were then harvested and used in 4 hr ^{51}Cr release assay or peptide recall assays.

^{51}Cr release assay

$HSV^{GM\text{-}CSF}$ treated PBMC (± NK depletion) or CTL were co-cultured with ^{51}Cr (Perkin-Elmer)-labelled MEL888, A375, MeWo or MCF-7 cells at different effector:target (E:T) ratios for 4 hrs (±2mM EGTA were indicated). Cells were then pelleted by centrifugation and 50µL of supernatant was transferred to scintillation plates (Perkin-Elmer) prior to analysis using a Wallac Jet 1459 Microbeta scintillation counter and Microbeta Windows software (Perkin-Elmer). Tumor cell % lysis was determined using the following calculation:

% lysis= (Sample CPM - Spontaneous CPM) / (Maximum CPM - Spontaneous CPM) x 100

Peptide Recall assay

To measure peptide specific CTL responses, autologous CD14+ cells were incubated with either melanocyte protein PMEL (PMEL), Tyrosinase (TYR) or Melanoma antigen recognized by T-cells 1 (Mart-1/MLANA) PepTivator peptide pools (15-mer peptide sequences with 11 amino acids overlap, Miltenyi Biotec) for 60 min at 37°C, according to the manufacturers' instructions. Autologous CD14+ cells, with or without peptide labelling, were then co-cultured with CTL for 60 min at 37°C before addition of Brefeldin A (1:1000, BioLegend) and an anti-CD8-APC antibody for identification of CTL. CTL were then incubated for a further 4 hrs at 37˚C and cells were fixed prior to intra-cellular IFNγ staining and acquisition/analysis by flow cytometry.

Statistical Significance

Statistical analysis was carried out with the Graphpad Prism software. Statistical differences among groups were determined using student's t-test, one-way ANOVA

or two-way ANOVA analysis. The criterion for statistical significance was p value less than 0.05.

Acknowledgements

The authors would like to thank Amgen for supplying the viruses used in this study. This research was also supported by the National Institute for Health Research (NIHR) infrastructure at Leeds. The views expressed are those of the author(s) and not necessarily those of the NHS, the NIHR or the Department of Health. The authors would also like to acknowledge Cancer Research UK (CRUK: C16708/A21855), Yorkshire Cancer Research (YCR; L374RA) and Kay Kendall Leukaemia Fund (KKLF; KKL1071) for financial support.

Conflicts of Interest, KJH and AAM have received consultancy fees and travel support from Amgen Inc.

Author Contribution

Conceptualization, F.E.M. and A.A.M.; Methodology, V.A.J.; Investigation, V.A.J., G.B.S., A.M.S.R., K.J.S., G.M., K.R.; Resources, B.K., O.D., H.P., D.D., A.S.; Writing - original draft, F.E.M., A.A.M and V.A.J.; Writing – review and editing, K.J.S. K.J.H., H.P., R.G.V.; Supervision, F.E.M., A.A.M. and V.A.J.; Funding acquisition, A.A.M.

References

1. Fountzilas C, Patel S, Mahalingam D. Review: Oncolytic virotherapy, updates and future directions. Oncotarget 2017;8(60):102617-39.

2. Sivendran S, Pan M, Kaufman HL, Saenger Y. Herpes simplex virus oncolytic vaccine therapy in melanoma. Expert opinion on biological therapy 2010;10(7):1145-53.

3. Donnelly OG, Errington-Mais F, Prestwich R, Harrington K, Pandha H, Vile R, et al. Recent Clinical Experience With Oncolytic Viruses. Current pharmaceutical biotechnology 2011.

4. Ribas A, Dummer R, Puzanov I, VanderWalde A, Andtbacka RHI, Michielin O, et al. Oncolytic Virotherapy Promotes Intratumoral T Cell Infiltration and Improves Anti-PD-1 Immunotherapy. Cell 2017;170(6):1109-19.e10.

5. Hu JC, Coffin RS, Davis CJ, Graham NJ, Groves N, Guest PJ, et al. A phase I study of OncoVEXGM-CSF, a second-generation oncolytic herpes simplex virus expressing granulocyte macrophage colony-stimulating factor. Clin Cancer Res 2006;12(22):6737-47.

6. Senzer NN, Kaufman HL, Amatruda T, Nemunaitis M, Reid T, Daniels G, et al. Phase II Clinical Trial of a Granulocyte-Macrophage Colony-Stimulating Factor-Encoding, Second-Generation Oncolytic Herpesvirus in Patients With Unresectable Metastatic Melanoma. J Clin Oncol 2009.

7. Kaufman HL, Kim DW, Deraffele G, Mitcham J, Coffin RS, Kim-Schulze S. Local and Distant Immunity Induced by Intralesional Vaccination with an Oncolytic Herpes Virus Encoding GM-CSF in Patients with Stage IIIc and IV Melanoma. Ann Surg Oncol 2010;17:718-30.

8. Kaufman HL, Bines SD. OPTIM trial: a Phase III trial of an oncolytic herpes virus encoding GM-CSF for unresectable stage III or IV melanoma. Future oncology 2010;6(6):941-9.

9. Andtbacka RH, Kaufman HL, Collichio F, Amatruda T, Senzer N, Chesney J, et al. Talimogene Laherparepvec Improves Durable Response Rate in Patients With Advanced Melanoma. J Clin Oncol 2015;33(25):2780-8.

10. Harrington KJ, Hingorani M, Tanay MA, Hickey J, Bhide SA, Clarke PM, et al. Phase I/II study of oncolytic HSV GM-CSF in combination with radiotherapy and cisplatin in untreated stage III/IV squamous cell cancer of the head and neck. Clin Cancer Res 2010;16(15):4005-15.

11. Chesney J, Puzanov I, Collichio F, Singh P, Milhem MM, Glaspy J, et al. Randomized, Open-Label Phase II Study Evaluating the Efficacy and Safety of Talimogene Laherparepvec in Combination With Ipilimumab Versus Ipilimumab Alone in Patients With Advanced, Unresectable Melanoma. Journal of clinical oncology : official journal of the American Society of Clinical Oncology 2018;36(17):1658-67.

12. Marks PA. The clinical development of histone deacetylase inhibitors as targeted anticancer drugs. Expert Opin Investig Drugs 2010;19(9):1049-66.

13. Conte M, De Palma R, Altucci L. HDAC inhibitors as epigenetic regulators for cancer immunotherapy. The international journal of biochemistry & cell biology 2018;98:65-74.

14. Suraweera A, O'Byrne KJ, Richard DJ. Combination Therapy With Histone Deacetylase Inhibitors (HDACi) for the Treatment of Cancer: Achieving the Full Therapeutic Potential of HDACi. Frontiers in oncology 2018;8:92.

15. Heers H, Stanislaw J, Harrelson J, Lee MW. Valproic acid as an adjunctive therapeutic agent for the treatment of breast cancer. European journal of pharmacology 2018;835:61-74.

16. Otsuki A, Patel A, Kasai K, Suzuki M, Kurozumi K, Antonio Chiocca E, et al. Histone Deacetylase Inhibitors Augment Antitumor Efficacy of Herpes-based Oncolytic Viruses. Mol Ther 2008;16:1546-55.

17. Nguyen TL, Wilson MG, Hiscott J. Oncolytic viruses and histone deacetylase inhibitors-A multi-pronged strategy to target tumor cells. Cytokine Growth Factor Rev 2010.

18. Jaime-Ramirez AC, Yu JG, Caserta E, Yoo JY, Zhang J, Lee TJ, et al. Reolysin and Histone Deacetylase Inhibition in the Treatment of Head and Neck Squamous Cell Carcinoma. Molecular therapy oncolytics 2017;5:87-96.

19. Bridle BW, Chen L, Lemay CG, Diallo JS, Pol J, Nguyen A, et al. HDAC inhibition suppresses primary immune responses, enhances secondary immune responses, and abrogates autoimmunity during tumor immunotherapy. Molecular therapy : the journal of the American Society of Gene Therapy 2013;21(4):887-94.

20. Marchini A, Scott EM, Rommelaere J. Overcoming Barriers in Oncolytic Virotherapy with HDAC Inhibitors and Immune Checkpoint Blockade. Viruses 2016;8(1).

21. Otsuki A, Patel A, Kasai K, Suzuki M, Kurozumi K, Antonio Chiocca E, et al. Histone Deacetylase Inhibitors Augment Antitumor Efficacy of Herpes-based Oncolytic Viruses. Molecular therapy : the journal of the American Society of Gene Therapy 2008;16(9):1546-55.

22. Li J, Bonifati S, Hristov G, Marttila T, Valmary-Degano S, Stanzel S, et al. Synergistic combination of valproic acid and oncolytic parvovirus H-1PV as a potential therapy against cervical and pancreatic carcinomas. EMBO molecular medicine 2013;5(10):1537-55.

23. Prestwich RJ, Errington F, Steele LP, Ilett EJ, Morgan RS, Harrington KJ, et al. Reciprocal human dendritic cell-natural killer cell interactions induce antitumor activity following tumor cell infection by oncolytic reovirus. J Immunol 2009;183(7):4312-21.

24. Adair RA, Scott KJ, Fraser S, Errington-Mais F, Pandha H, Coffey M, et al. Cytotoxic and immune-mediated killing of human colorectal cancer by reovirus-loaded blood and liver mononuclear cells. Int J Cancer 2012.

25. Parrish C, Scott GB, Migneco G, Scott KJ, Steele LP, Ilett E, et al. Oncolytic reovirus enhances rituximab-mediated antibody-dependent cellular cytotoxicity against chronic lymphocytic leukaemia. Leukemia 2015.

26. Prestwich RJ, Errington F, Ilett EJ, Morgan RS, Scott KJ, Kottke T, et al. Tumor infection by oncolytic reovirus primes adaptive antitumor immunity. Clinical cancer research : an official journal of the American Association for Cancer Research 2008;14(22):7358-66.

27. Prestwich RJ, Ilett EJ, Errington F, Diaz RM, Steele LP, Kottke T, et al. Immune-Mediated Antitumor Activity of Reovirus Is Required for Therapy and Is Independent of Direct Viral Oncolysis and Replication. Clinical Cancer Research 2009;15:4374-81.

28. Parrish C, Scott GB, Migneco G, Scott KJ, Steele LP, Ilett E, et al. Oncolytic reovirus enhances rituximab-mediated antibody-dependent cellular

cytotoxicity against chronic lymphocytic leukaemia. Leukemia 2015;29(9):1799-810.

29. Errington F, White CL, Twigger KR, Rose A, Scott K, Steele L, et al. Inflammatory tumour cell killing by oncolytic reovirus for the treatment of melanoma. Gene therapy 2008;15(18):1257-70.

30. Errington F, Steele L, Prestwich R, Harrington KJ, Pandha HS, Vidal L, et al. Reovirus activates human dendritic cells to promote innate antitumor immunity. Journal of immunology (Baltimore, Md : 1950) 2008;180(9):6018-26.

31. Poggi A, Catellani S, Garuti A, Pierri I, Gobbi M, Zocchi MR. Effective in vivo induction of NKG2D ligands in acute myeloid leukaemias by all-trans-retinoic acid or sodium valproate. Leukemia 2009;23(4):641-8.

32. Diermayr S, Himmelreich H, Durovic B, Mathys-Schneeberger A, Siegler U, Langenkamp U, et al. NKG2D ligand expression in AML increases in response to HDAC inhibitor valproic acid and contributes to allorecognition by NK-cell lines with single KIR-HLA class I specificities. Blood 2008;111(3):1428-36.

33. Alvarez-Breckenridge CA, Yu J, Price R, Wei M, Wang Y, Nowicki MO, et al. The histone deacetylase inhibitor valproic acid lessens NK cell action against oncolytic virus-infected glioblastoma cells by inhibition of STAT5/T-BET signaling and generation of gamma interferon. J Virol 2012;86(8):4566-77.

34. Liu BL, Robinson M, Han ZQ, Branston RH, English C, Reay P, et al. ICP34.5 deleted herpes simplex virus with enhanced oncolytic, immune stimulating, and anti-tumour properties. Gene Ther 2003;10(4):292-303.

35. Taipale K, Liikanen I, Juhila J, Turkki R, Tahtinen S, Kankainen M, et al. Chronic Activation of Innate Immunity Correlates With Poor Prognosis in Cancer Patients Treated With Oncolytic Adenovirus. Molecular therapy : the journal of the American Society of Gene Therapy 2016;24(1):175-83.

36. Alvarez-Breckenridge CA, Yu J, Price R, Wojton J, Pradarelli J, Mao H, et al. NK cells impede glioblastoma virotherapy through NKp30 and NKp46 natural cytotoxicity receptors. Nature medicine 2012;18(12):1827-34.

37. Tai LH, Auer R. Attacking Postoperative Metastases using Perioperative Oncolytic Viruses and Viral Vaccines. Front Oncol 2014;4:217.

38. Thirion G, Saxena A, Hulhoven X, Markine-Goriaynoff D, Van Snick J, Coutelier JP. Modulation of the host microenvironment by a common non-oncolytic mouse virus leads to inhibition of plasmacytoma development through NK cell activation. The Journal of general virology 2014;95(Pt 7):1504-9.

39. Zamarin D, Holmgaard RB, Subudhi SK, Park JS, Mansour M, Palese P, et al. Localized oncolytic virotherapy overcomes systemic tumor resistance to immune checkpoint blockade immunotherapy. Science translational medicine 2014;6(226):226ra32.

40. Kottke T, Chester J, Ilett E, Thompson J, Diaz R, Coffey M, et al. Precise scheduling of chemotherapy primes VEGF-producing tumors for successful systemic oncolytic virotherapy. Molecular therapy : the journal of the American Society of Gene Therapy 2011;19(10):1802-12.

41. Cerullo V, Diaconu I, Romano V, Hirvinen M, Ugolini M, Escutenaire S, et al. An oncolytic adenovirus enhanced for toll-like receptor 9 stimulation increases

antitumor immune responses and tumor clearance. Molecular therapy : the journal of the American Society of Gene Therapy 2012;20(11):2076-86.

42. Miller CG, Fraser NW. Requirement of an integrated immune response for successful neuroattenuated HSV-1 therapy in an intracranial metastatic melanoma model. Molecular therapy : the journal of the American Society of Gene Therapy 2003;7(6):741-7.

43. Samudio I, Rezvani K, Shaim H, Hofs E, Ngom M, Bu L, et al. UV-inactivated HSV-1 potently activates NK cell killing of leukemic cells. Blood 2016.

44. Ohkusu-Tsukada K, Ohta S, Kawakami Y, Toda M. Adjuvant effects of formalin-inactivated HSV through activation of dendritic cells and inactivation of myeloid-derived suppressor cells in cancer immunotherapy. International journal of cancer 2011;128(1):119-31.

45. Schwaiger T, Knittler MR, Grund C, Roemer-Oberdoerfer A, Kapp JF, Lerch MM, et al. Newcastle disease virus mediates pancreatic tumor rejection via NK cell activation and prevents cancer relapse by prompting adaptive immunity. International journal of cancer 2017;141(12):2505-16.

46. Samson A, Bentham MJ, Scott K, Nuovo G, Bloy A, Appleton E, et al. Oncolytic reovirus as a combined antiviral and anti-tumour agent for the treatment of liver cancer. Gut 2018;67(3):562-73.

47. Yoneyama H, Matsuno K, Toda E, Nishiwaki T, Matsuo N, Nakano A, et al. Plasmacytoid DCs help lymph node DCs to induce anti-HSV CTLs. The Journal of experimental medicine 2005;202(3):425-35.

48. Schuster P, Thomann S, Werner M, Vollmer J, Schmidt B. A subset of human plasmacytoid dendritic cells expresses CD8alpha upon exposure to herpes simplex virus type 1. Frontiers in microbiology 2015;6:557.

49. Kawamura K, Kadowaki N, Kitawaki T, Uchiyama T. Virus-stimulated plasmacytoid dendritic cells induce CD4+ cytotoxic regulatory T cells. Blood 2006;107(3):1031-8.

50. Marks PA. Histone deacetylase inhibitors: a chemical genetics approach to understanding cellular functions. Biochimica et biophysica acta 2010;1799(10-12):717-25.

51. Katsura T, Iwai S, Ota Y, Shimizu H, Ikuta K, Yura Y. The effects of trichostatin A on the oncolytic ability of herpes simplex virus for oral squamous cell carcinoma cells. Cancer gene therapy 2009;16(3):237-45.

52. Nevels M, Nitzsche A, Paulus C. How to control an infectious bead string: nucleosome-based regulation and targeting of herpesvirus chromatin. Rev Med Virol 2011;21(3):154-80.

53. Smiley JR. Herpes simplex virus virion host shutoff protein: immune evasion mediated by a viral RNase? Journal of virology 2004;78(3):1063-8.

54. Dauber B, Saffran HA, Smiley JR. The herpes simplex virus 1 virion host shutoff protein enhances translation of viral late mRNAs by preventing mRNA overload. Journal of virology 2014;88(17):9624-32.

55. Cliffe AR, Knipe DM. Herpes simplex virus ICP0 promotes both histone removal and acetylation on viral DNA during lytic infection. Journal of virology 2008;82(24):12030-8.

56. Riker RR, Gagnon DJ, Hatton C, May T, Seder DB, Stokem K, et al. Valproate Protein Binding Is Highly Variable in ICU Patients and Not Predicted by Total Serum Concentrations: A Case Series and Literature Review. Pharmacotherapy 2017;37(4):500-08.

57. Ghannoum M, Laliberte M, Nolin TD, MacTier R, Lavergne V, Hoffman RS, et al. Extracorporeal treatment for valproic acid poisoning: systematic review and recommendations from the EXTRIP workgroup. Clinical toxicology (Philadelphia, Pa) 2015;53(5):454-65.

58. Kawakami Y, Eliyahu S, Delgado CH, Robbins PF, Rivoltini L, Topalian SL, et al. Cloning of the gene coding for a shared human melanoma antigen recognized by autologous T cells infiltrating into tumor. Proceedings of the National Academy of Sciences of the United States of America 1994;91(9):3515-9.

59. Sheridan JW, Simmons RJ. Studies on a human melanoma cell line: effect of cell crowding and nutrient depletion on the biophysical and kinetic characteristics of the cells. Journal of cellular physiology 1981;107(1):85-100.

Figure Legends

Figure 1. $HSV^{GM\text{-}CSF}$ induces innate and adaptive anti-tumor immunity. A. Healthy donor PBMC (±$HSV^{GM\text{-}CSF}$ treatment) were co-cultured with melanoma targets and NK cell ($CD56^+/CD3^-$) CD107 degranulation was determined by flow cytometry. The mean percentage of NK cells degranulating after co-culture with MEL888, A375 and MeWo tumor cell targets +SEM is shown (at least n=4). **B**. PBMC from melanoma patients with metastatic disease (± $HSV^{GM\text{-}CSF}$ treatment) were co-cultured with melanoma targets (MEL888) and NK cell ($CD56^+/CD3^-$) CD107 degranulation was determined by flow cytometry. The mean percentage of NK cells expressing CD107, +SEM, is shown (n=4). **C**. Healthy donor PBMC (±$HSV^{GM\text{-}CSF}$) were co-cultured with MEL888, A375 and MeWo cell targets and the % of tumor cell lysis was determined by ^{51}Cr release. Graph shows the mean of at least three experiments ±SEM. **D**. Immature dendritic cells were treated with ±$HSV^{GM\text{-}CSF}$ for 48h, cell surface expression of CD86, CD80, HLA-ABC and HLA-DR/DP/DQ was determined by flow cytometry. Representative histograms (top panel) and the mean fold increase in expression compared to isotype controls +SEM (bottom panel) are shown (n=4). **E**. Supernatants from melanoma cells treated with ±$HSV^{GM\text{-}CSF}$ and co-cultured with iDC were collected and concentrations of GM-CSF, IL-10 and TNFα were determined by ELISA. Graph shows the mean +SEM (n=3). **F**. MEL888 cells were either left untreated (Mel888-primed CTL) or treated with 0.1 pfu/cell $HSV^{GM\text{-}CSF}$ (Mel888+HSV-GMCSF-primed CTL) and cultured with iDC for 24h before non-adherent cells were removed and cultured with autologous PBMC. CTL were re-stimulated once (as appropriate) and then used in 4h ^{51}Cr release assays against

MEL888 (relevant) or MCF-7 (irrelevant) targets. The graph shows the mean percentage of tumor cell death ±SEM (n=3). Statistical significance is denoted by *p<0.05, **p<0.01, p***< 0.005.

Figure 2. Innate activation is dependent on type I IFNs and CD14^{+} monocytes. **A**. Healthy donor PBMC or isolated NK cells (±HSV$^{GM\text{-}CSF}$ treatment) were co-cultured with melanoma targets and NK cell (CD56^{+}/CD3^{-}): **(i)** CD69 expression and **(ii)** CD107 degranulation were determined by flow cytometry (n=4). **B**. Healthy donor PBMC were treated with HSV$^{GM\text{-}CSF}$ for 48hrs and the production of IFNγ, IFNα, IFNβ, and IL-29 was determined by ELISA. Graph shows the mean of at least four independent experiments ±SEM. **C**. Healthy donor PBMC were treated overnight with HSV$^{GM\text{-}CSF}$ either alone or in the presence of IFNα/β blocking antibodies/isotype controls before: **(i)** CD69 upregulation on CD56^{+}/CD3^{-} NK cells was determined by flow cytometry. Graph shows the average percentage of NK cells expressing CD69, + SEM (n=3); **(ii)** PBMC (±IFN blockade and ± HSV$^{GM\text{-}CSF}$) were co-cultured with MEL888 cells and NK cell CD107 degranulation was determined by flow cytometry. Graph shows the mean percentage of NK cells expressing CD107a/b, +SEM (n=3); and **(iii)** PBMC (±IFN blockade and ± HSV$^{GM\text{-}CSF}$) were co-cultured with MEL888 at indicated E:T ratios and % tumor cell lysis determined by ^{51}Cr release. Graph shows the mean percentage lysis, ±SEM (n=3). **D**. IFNα/β production from whole PBMC, or CD14^{+} monocyte-depleted PBMC was determined by ELISA. Graph shows the mean, +SEM (n=5). Statistical significance is denoted by *p<0.05, **p<0.01, p***< 0.005.

Figure 3. VPA enhances HSV$^{GM\text{-}CSF}$-induced cytotoxicity, viral replication and transgene expression. **A.** Melanoma cell lines were seeded and treated with VPA

(0, 1 and 2 mM) for 24hrs prior to the addition of $HSV^{GM\text{-}CSF}$ at concentrations ranging from 0 to 1pfu/cell. Cells were left for a further 48hrs and cell viability was determined by MTT assay. Graph shows the average cell viability for at least five independent experiments ±SEM. **B**. VPA-treated melanoma cells were treated with $HSV^{GM\text{-}CSF}$ for 24hrs and GM-CSF production was determined by ELISA. Graph shows the mean, +SEM (n=6). **C**. MEL888 or A375 cells were treated with 0.05pfu/cell $HSV^{GM\text{-}CSF}$ alone, 1mM VPA for 24hrs prior to 0.05pfu/cell $HSV^{GM\text{-}CSF}$ or 1mM VPA/0.05pfu/cell $HSV^{GM\text{-}CSF}$ simultaneously. Cells were left for 24hrs and fold increase in $HSV^{GM\text{-}CSF}$ replication was determined by plaque assay. Graph shows the mean, +SEM (n=4). Statistical significance is denoted by *p<0.05, **p<0.01, p***< 0.005, ****p<0.0001.

Figure 4. VPA augments $HSV^{GM\text{-}CSF}$ innate anti-tumor immunity. A. Expression of NK ligands (MICA/B and ULBP2/5/6) on the surface of melanoma cells was determined by flow cytometry. Cells were treated with VPA at indicated doses for 48hr. Mean fluorescence intensity is shown, +SEM (n=3). **B**. Healthy donor PBMC (untreated (0 pfu) or activated with $HSV^{GM\text{-}CSF}$ (0.001 or 0.01 pfu) overnight) were co-cultured with melanoma cells ±VPA for 5hrs and the % target cell death was determined by flow cytometry. The graph shows the mean, +SEM, for at least four independent experiments. Statistical significance is denoted by *p<0.05, **p<0.01, p***< 0.005.

Figure 5: VPA enhances $HSV^{GM\text{-}CSF}$ CTL responses against Melanoma. (A-C) MEL888 cells were treated with indicated doses of VPA for 24h followed by $HSV^{GM\text{-}CSF}$ (0.1 pfu/cell) and co-cultured with iDC for 24h, non-adherent cells (containing tumor-loaded APC) were removed and cultured with autologous PBMC for 7 days. CTL cultures were re-stimulated appropriately then used in TAA peptide recall

assays. **A**. Graph shows the mean (%) of IFNγ+ CD8+ T cells following indicated peptide recall (n=4). **B**. Cell-free supernatants from VPA-treated, $HSV^{GM\text{-}CSF}$-infected MEL888 cells following co-cultured with iDC were collected and concentrations of IL-10 were determined by ELISA. Graph shows the mean, +SEM (n=3). **C**. Cell-free supernatants from CTL cultures were collected at day 14 and concentrations of IFNγ were determined by ELISA. Graph shows the mean, +SEM (n=4). **(D-F)** A375 cells were treated with indicated doses of VPA for 24h alone **(D)** or VPA followed by $HSV^{GM\text{-}CSF}$ at indicated doses **(E-F)**. **D**. PMEL mRNA expression levels were quantified by qRT-PCR relative to EF1α housekeeping control following treatment with VPA for 24hrs (n=6). **E**. Intracellular protein expression of PMEL was quantified by: **(i)** flow cytometry (±VPA and/or ± $HSV^{GM\text{-}CSF}$); graph shows the mean fluorescence intensity +SEM, (n=3), or **(ii)** immunofluorescence (±VPA and 0.1pfu/cell $HSV^{GM\text{-}CSF}$). **F**. A375 cells were treated with indicated doses of VPA for 24h followed by $HSV^{GM\text{-}CSF}$ (0.1 pfu/cell) and co-cultured with iDC for 24h, non-adherent cells (containing tumor-loaded APC) were removed and cultured with autologous PBMC for 7 days. CTL cultures were re-stimulated appropriately then used in a PMEL peptide recall assay. Graph shows the mean (%) IFNγ+ CD8+ T cells, +SEM (n=2). Statistical significance is denoted by *$p<0.05$, **$p<0.01$.

Figure 1

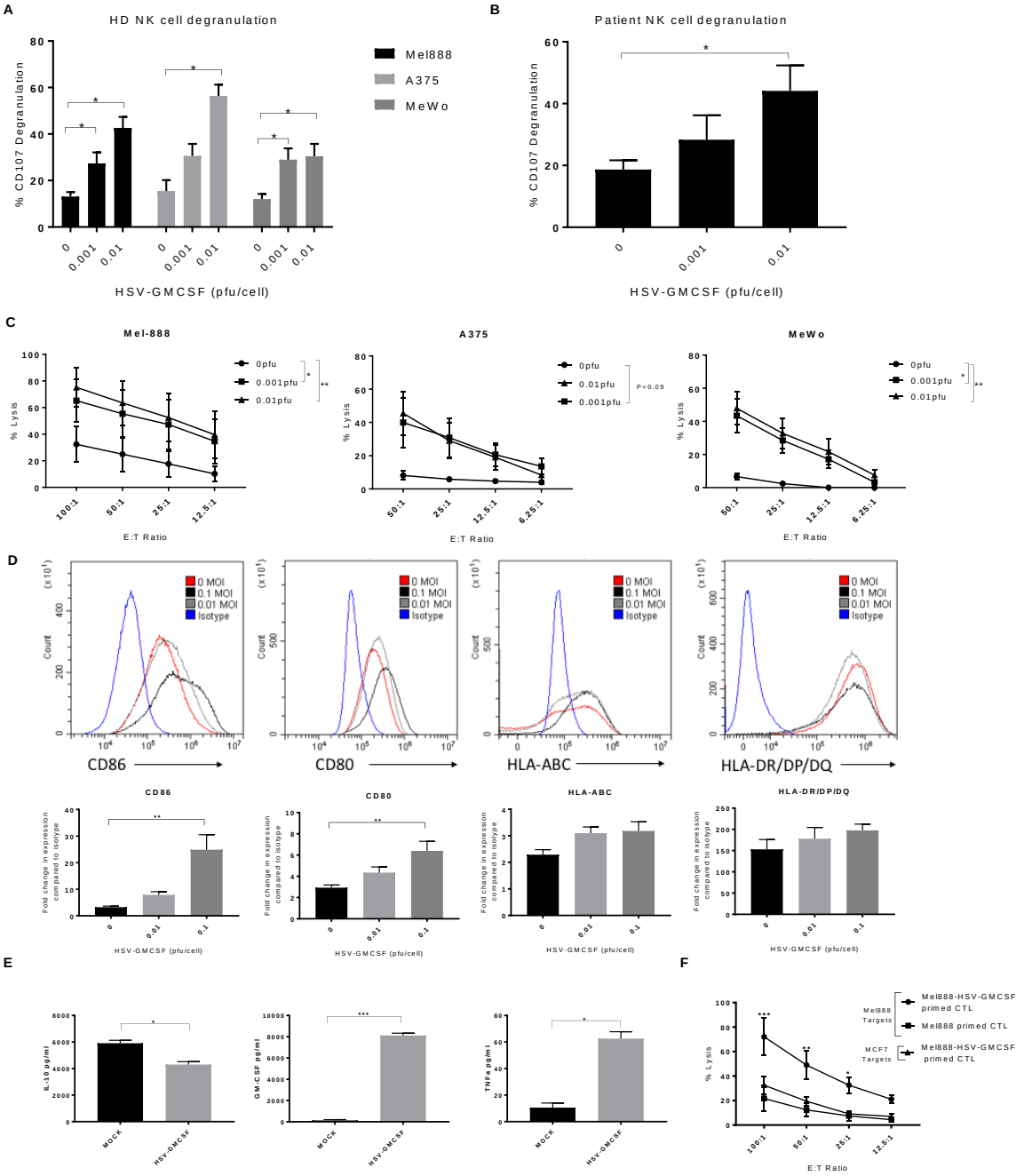
A
HD NK cell degranulation
% CD107 Degranulation
Mel888
A375
MeWo
HSV-GMCSF (pfu/cell)
B
Patient NK cell degranulation
% CD107 Degranulation
HSV-GMCSF (pfu/cell)
C
Mel-888
A375
MeWo
% Lysis
0pfu
0.001pfu
0.01pfu
P=0.09
E:T Ratio
D
0 MOI
0.1 MOI
0.01 MOI
Isotype
Count
CD86
CD80
HLA-ABC
HLA-DR/DP/DQ
Fold change in expression compared to isotype
HSV-GMCSF (pfu/cell)
E
IL-10 pg/ml
GM-CSF pg/ml
TNFa pg/ml
MOCK
HSV-GMCSF
F
% Lysis
Mel888 Targets
MCF7 Targets
Mel888-HSV-GMCSF primed CTL
Mel888 primed CTL
Mel888-HSV-GMCSF primed CTL
E:T Ratio

Figure 2

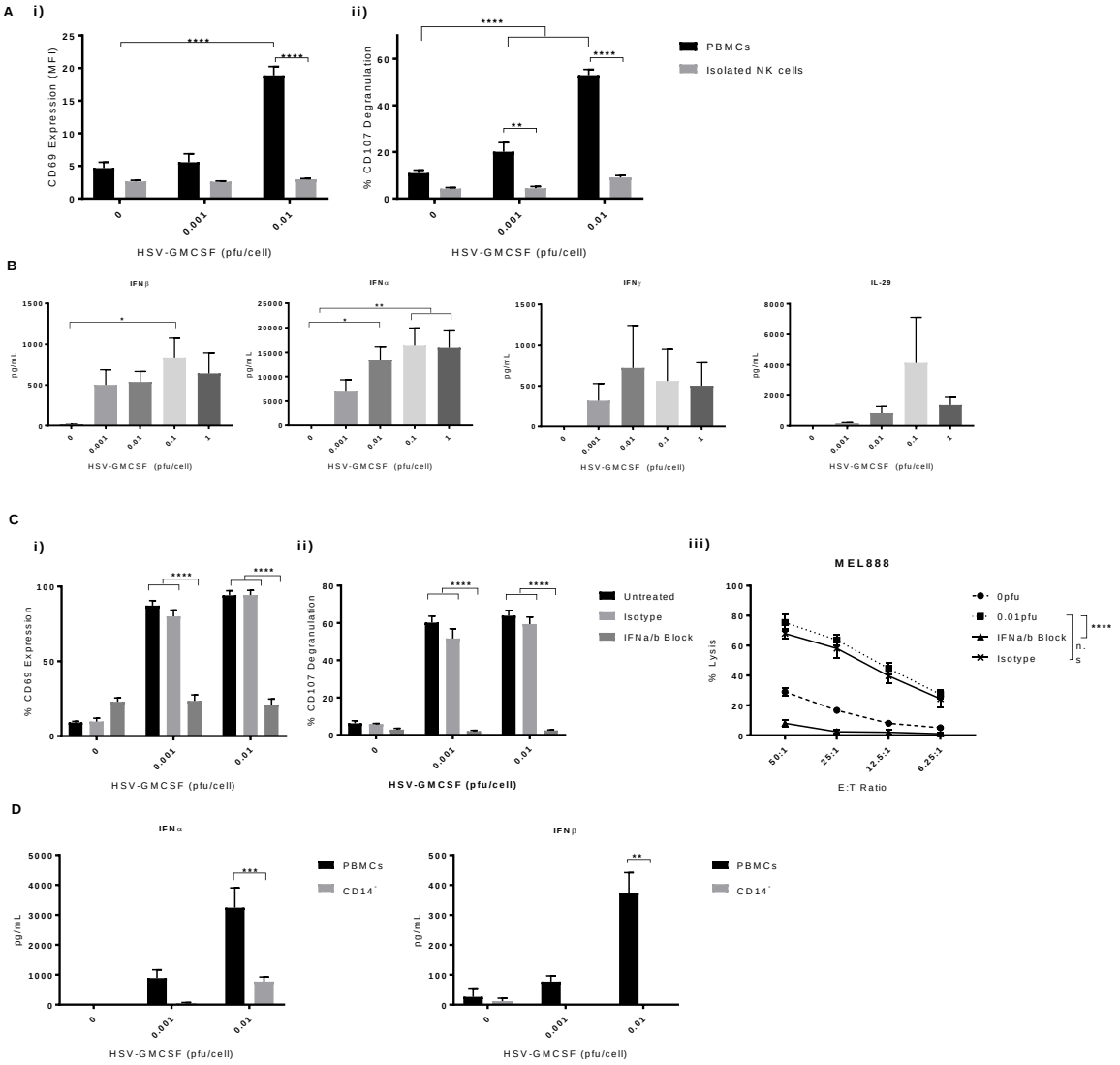
A
i)
ii)
CD69 Expression (MFI)
% CD107 Degranulation
HSV-GMCSF (pfu/cell)
PBMCs
Isolated NK cells
B
IFNβ
IFNα
IFNγ
IL-29
pg/mL
HSV-GMCSF (pfu/cell)
C
i)
ii)
iii)
% CD69 Expression
% CD107 Degranulation
HSV-GMCSF (pfu/cell)
Untreated
Isotype
IFNa/b Block
MEL888
% Lysis
E:T Ratio
0pfu
0.01pfu
IFNa/b Block
Isotype
n.s
D
IFNα
IFNβ
pg/mL
PBMCs
CD14-
HSV-GMCSF (pfu/cell)

Figure 3

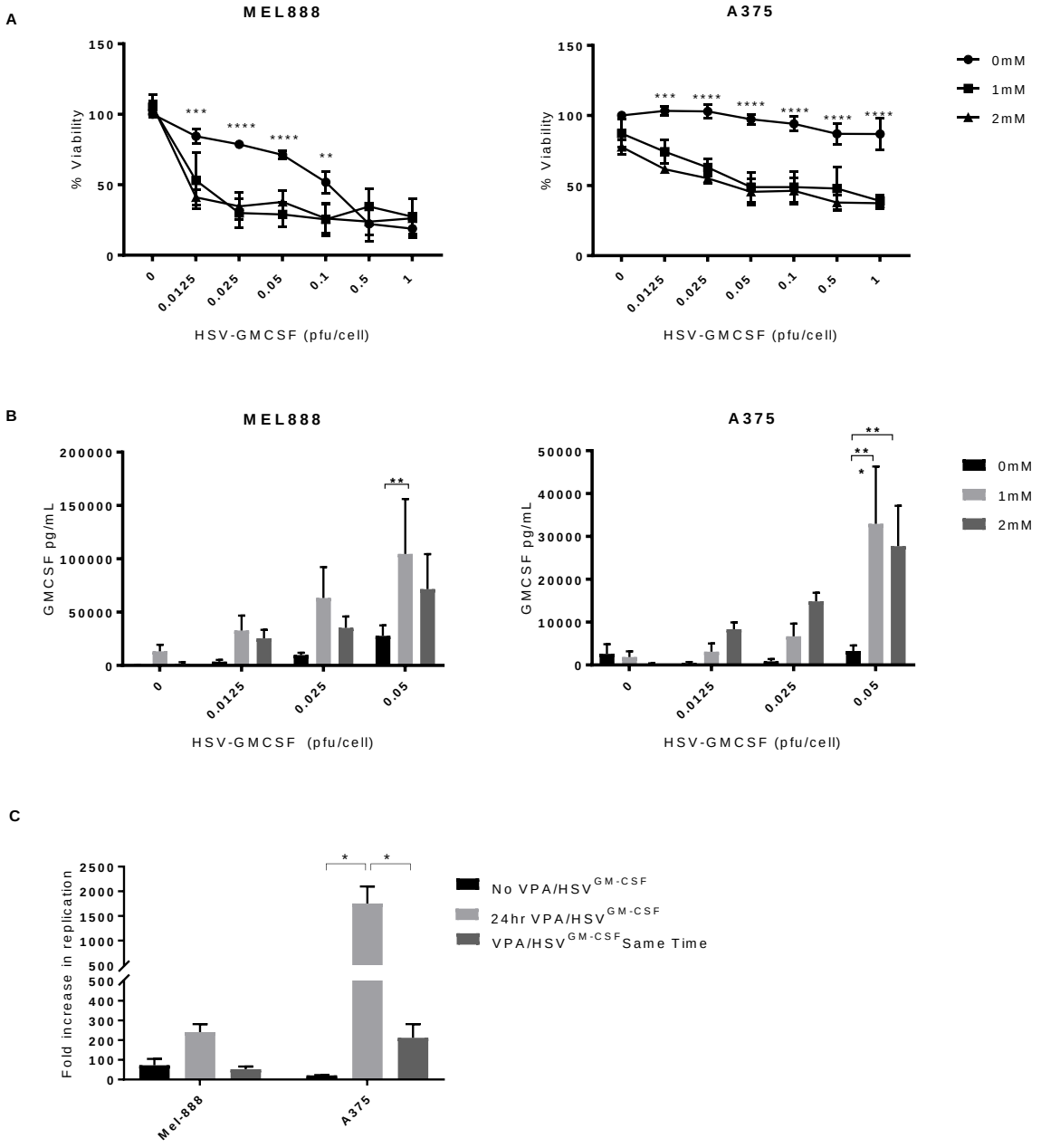
A
MEL888
A375
% Viability
HSV-GMCSF (pfu/cell)
0mM
1mM
2mM
B
MEL888
A375
GMCSF pg/mL
HSV-GMCSF (pfu/cell)
0mM
1mM
2mM
C
Fold increase in replication
Mel-888
A375
No VPA/HSV GM-CSF
24hr VPA/HSV GM-CSF
VPA/HSV GM-CSF Same Time

Figure 4

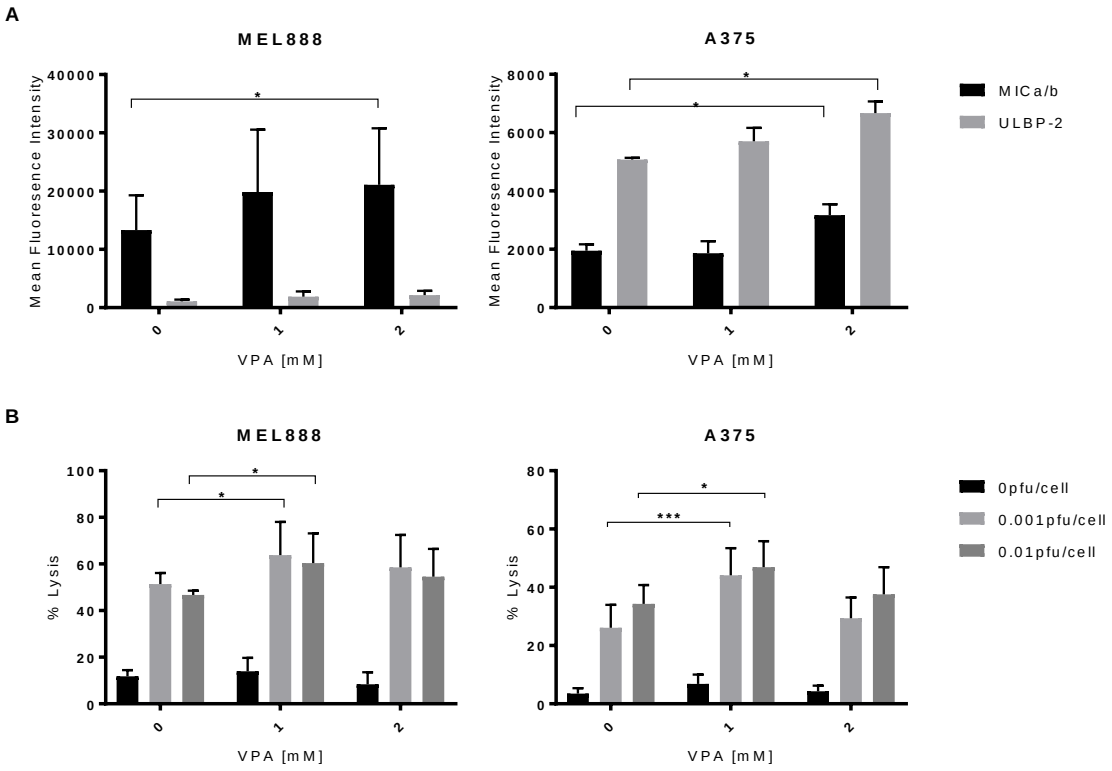
A
MEL888
A375
Mean Fluoresence Intensity
40000
30000
20000
10000
0
8000
6000
4000
2000
VPA [mM]
MICa/b
ULBP-2
B
% Lysis
100
80
60
40
20
***
0pfu/cell
0.001pfu/cell
0.01pfu/cell

Figure 5

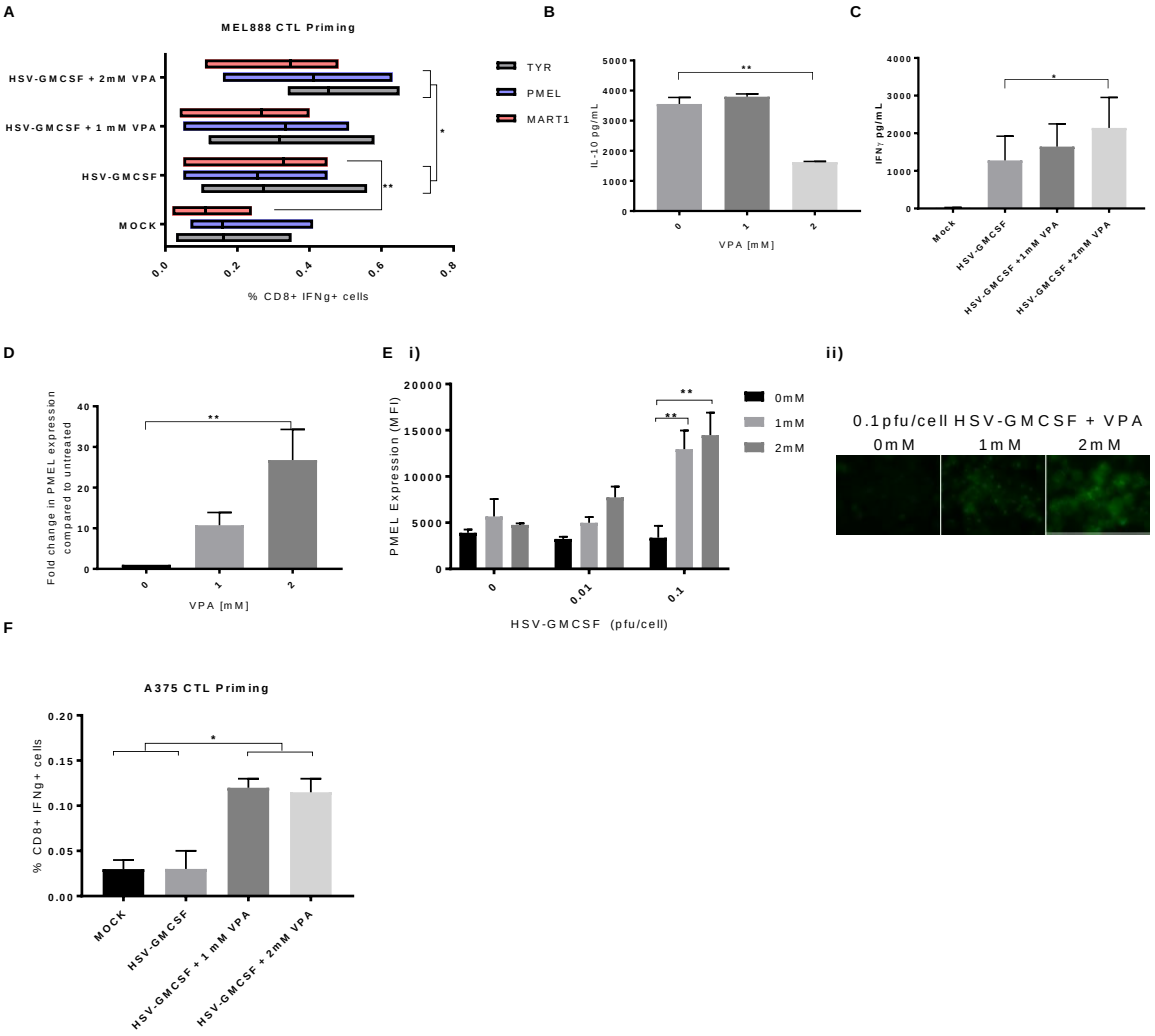
A
MEL888 CTL Priming
HSV-GMCSF + 2mM VPA
HSV-GMCSF + 1 mM VPA
HSV-GMCSF
MOCK
% CD8+ IFNg+ cells
B
TYR
PMEL
MART1
IL-10 pg/mL
VPA [mM]
C
IFNγ pg/mL
Mock
HSV-GMCSF
HSV-GMCSF +1mM VPA
HSV-GMCSF +2mM VPA
D
Fold change in PMEL expression compared to untreated
VPA [mM]
E i)
PMEL Expression (MFI)
0mM
1mM
2mM
HSV-GMCSF (pfu/cell)
ii)
0.1pfu/cell HSV-GMCSF + VPA
0mM
1mM
2mM
F
A375 CTL Priming
% CD8+ IFNg+ cells
MOCK
HSV-GMCSF
HSV-GMCSF + 1 mM VPA
HSV-GMCSF + 2mM VPA

Supplementary Figures

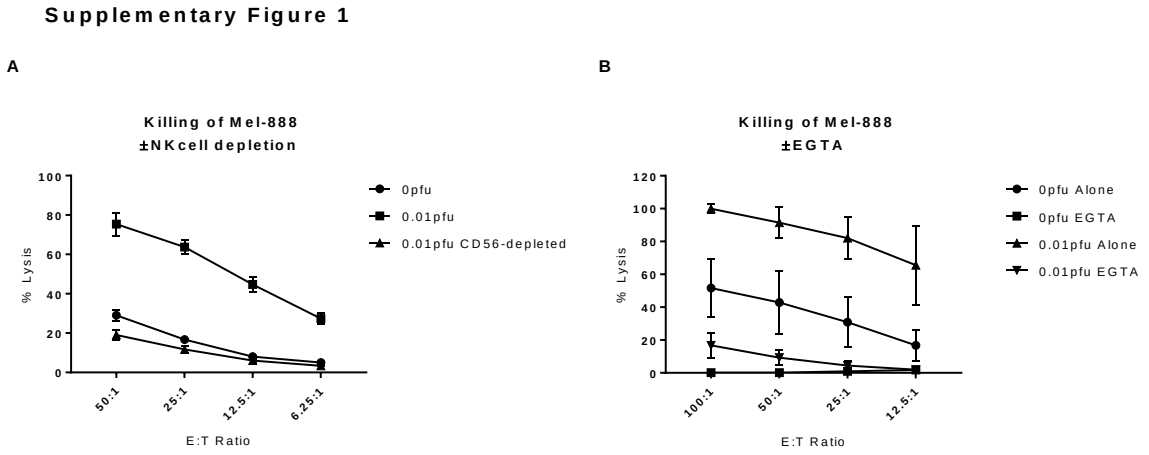

Supplementary Figure 1. NK cells are responsible for lysis of MEL888 target cells. **A**. PBMC were either left untreated (0 pfu/cell) or treated with 0.01pfu/cell $HSV^{GM\text{-}CSF}$ overnight, before PBMC were then either left intact (0.01pfu) or NK cells were depleted using $CD56^{+}$ MACS selection (0.01pfu CD56-depleted) prior to ^{51}Cr release assays. The mean percentage lysis of ^{51}Cr-labelled MEL888 tumor cell targets is shown (n=3; ±SEM). **B**. PBMC were either left untreated (0 pfu/cell) or treated with 0.01pfu/cell $HSV^{GM\text{-}CSF}$ overnight. Percentage lysis of ^{51}Cr-labelled MEL888 targets was determined in the presence or absence of 2mM EGTA (n=2, ±SEM).

Supplementary Figure 2

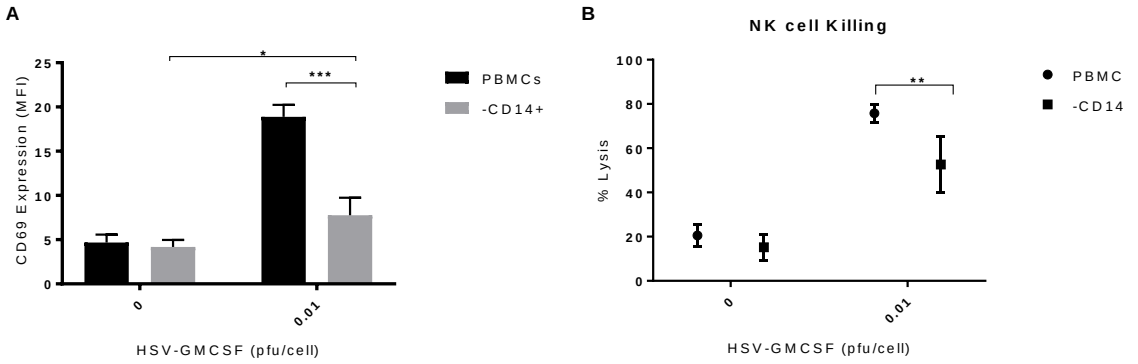

Supplementary Figure 2. Depletion of CD14+monocytes from PBMC decreases NK cell activation. **A**. Heathy donor PBMC (±$CD14^+$ monocyte depletion) were treated with $HSV^{GM\text{-}CSF}$ overnight and the expression of CD69 on NK cells was determined by flow cytometry. Data shows the average mean fluorescence intensity of CD69 expression on NK cells (n=4, +SEM). **B**. Heathy donor PBMC (±$CD14^+$ monocyte depletion) were treated with $HSV^{GM\text{-}CSF}$ overnight, co-cultured with MEL888 cells for 4hrs, and target cell lysis was determined by ^{51}Cr release. Data shows the average percentage tumor cell lysis (n=4, ±SEM).

Supplementary Figure 3

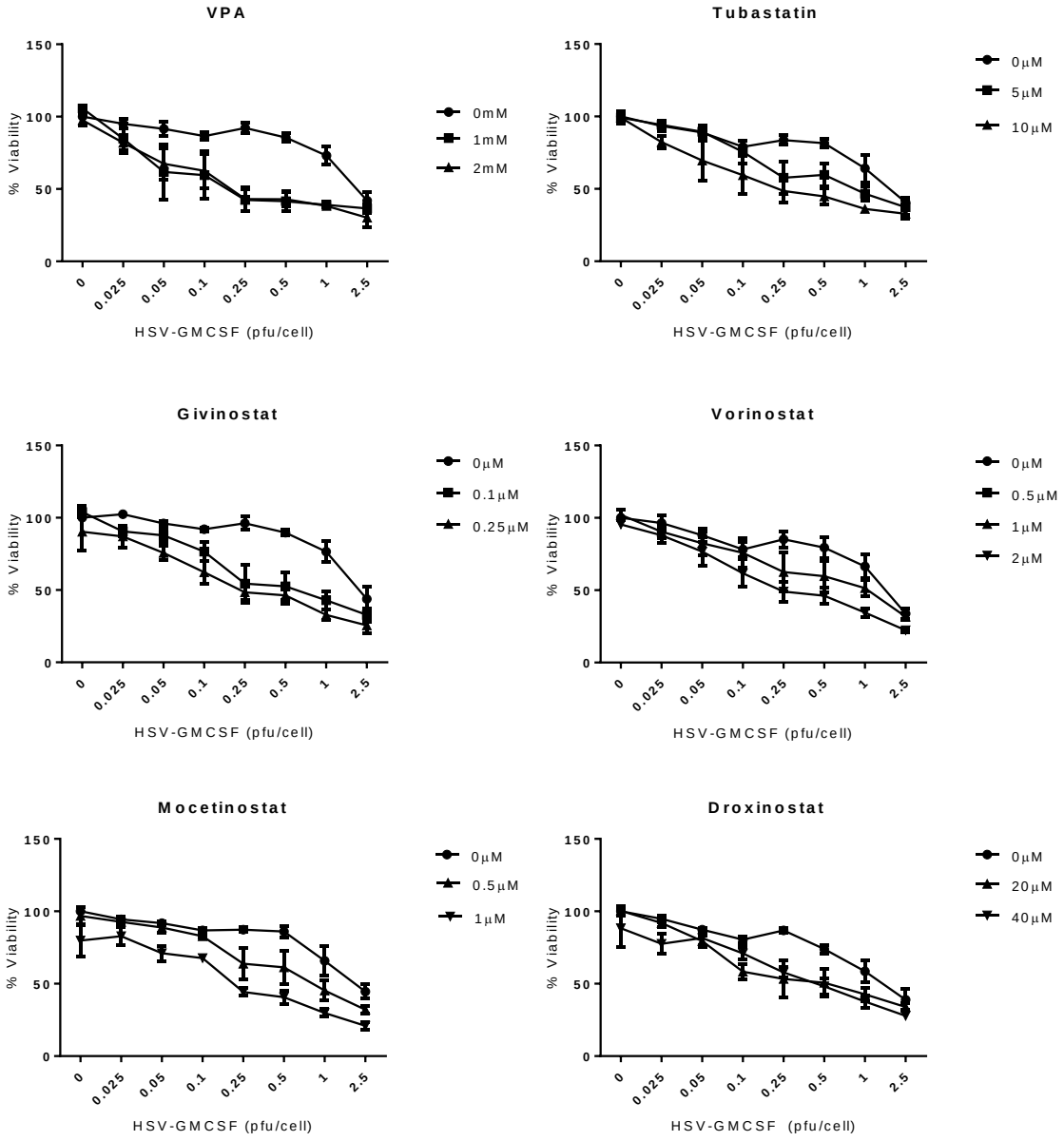

Supplementary Figure 3. Multiple HDACi enhance HSV$^{GM\text{-}CSF}$-induced cytotoxicity. Melanoma cell lines were seeded and treated with a range of HDACi at sub toxic doses for 24hrs, prior to the addition of HSV$^{GM\text{-}CSF}$ at concentrations ranging from 0 to 2.5pfu/cell. Cells were left for a further 48hrs and cell viability was determined by MTT assay. Data shown is the average of at least three independent experiments, ±SEM.

Supplementary Figure 4

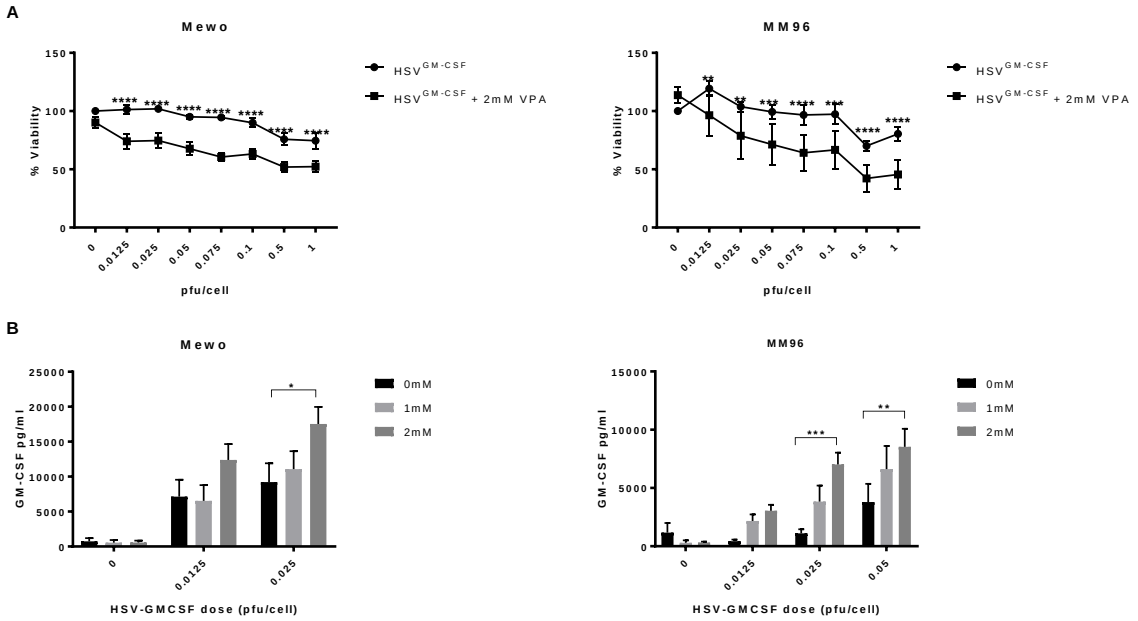

Supplementary Figure 4: VPA enhances HSV^{GMCSF} cytotoxicity and transgene expression. A. Melanoma cell lines (MeWo and MM96) were seeded and treated with VPA for 24hrs prior to the addition of HSV$^{GM\text{-}CSF}$ at concentrations ranging from 0 to 1pfu/cell. Cells were left for a further 48hrs and cell viability was determined by MTT assay. Data shown is the average of at least four independent experiments ±SEM. **B**. VPA-treated cells were treated with HSV$^{GM\text{-}CSF}$ for 24hrs and GM-CSF production was determined by ELISA. Data shows the mean of at least five independent experiments +SEM. Statistical significance is denoted by *p<0.05, **p<0.01, p***< 0.005, ****p<0.0001.

Supplementary Figure 5

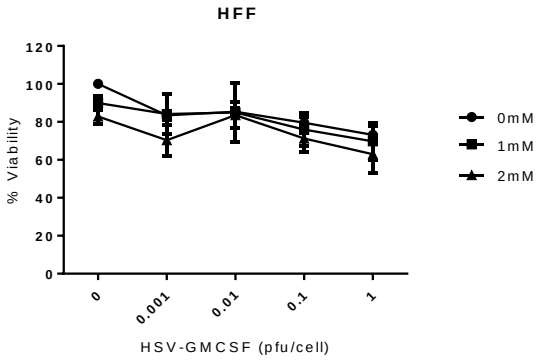

Supplementary Figure 5. VPA does not enhance HSV$^{GM\text{-}CSF}$ cytotoxicity in normal HFF. HFF were seeded and treated with 0, 1 or 2mM VPA for 24hrs, prior to the addition of HSV$^{GM\text{-}CSF}$ at concentrations ranging from 0 to 1pfu/cell. Cells were left for a further 48hrs and cell viability was determined by MTT assay (n=3, ±SEM).

Supplementary Figure 6

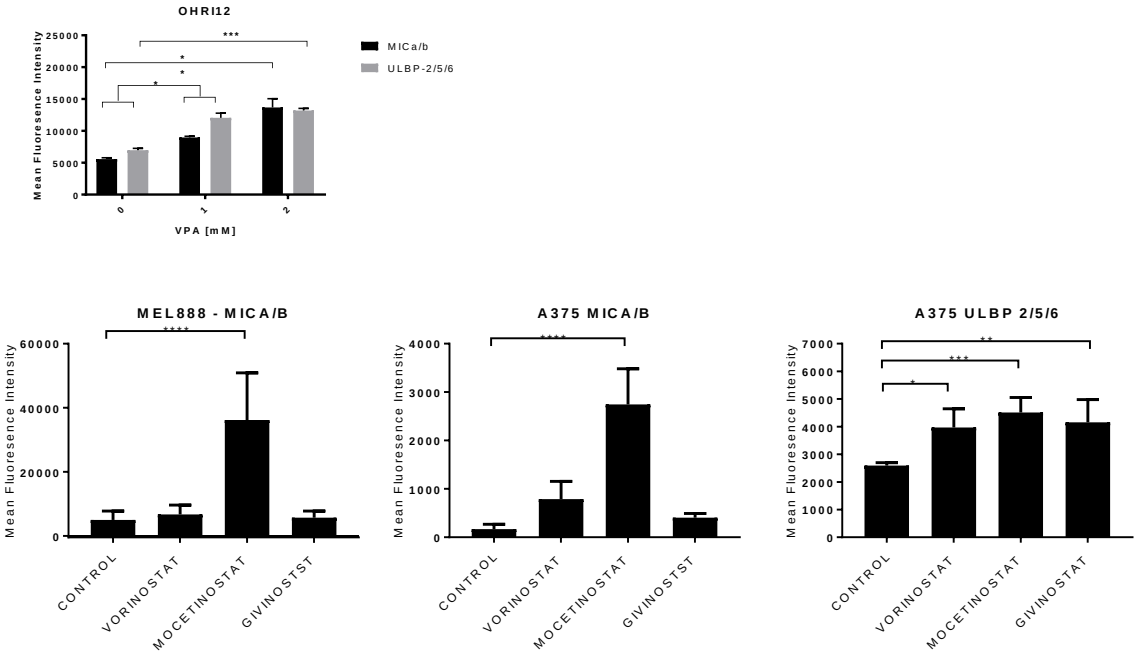

Supplementary Figure 6: VPA up-regulates NK cell activatory ligands on primary melanoma cells and alternative HDACi modulate MICA/B and ULBP2/5/6 expression. A. Expression of NK ligands (MICA/B and ULBP2/5/6) on the surface of primary melanoma cells (OHRI12) was determined by flow cytometry. Cells were treated with VPA at indicated doses for 48hr (n=3, +SEM). **B**. MEL888 and A375 cells were treated with 2mM VPA, 2µM vorinostat, 1µM mocetinostat and 0.2µM givinostat for 48hrs and the expression of MICA/B and ULBP2/5/6 was determined by flow cytometry (n=3, +SEM).

Supplementary Figure 7

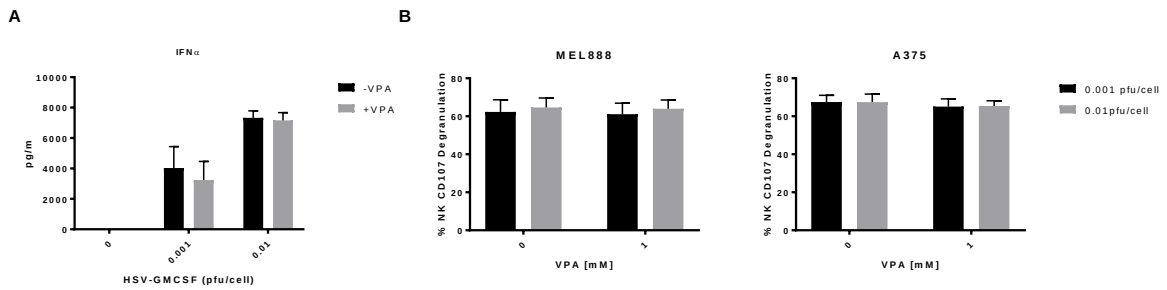

Supplementary Figure 7. Pre-treatment of PBMC with VPA does not prevent IFNα production or NK cell activation. **A**. IFNα production from PBMC pre-treated ±VPA for 4 hrs followed by $HSV^{GM\text{-}CSF}$ treatment (0, 0.01 and 0.001pfu/cell) overnight was determined by ELISA (n=3, +SEM); un-bound VPA was removed prior to addition of $HSV^{GM\text{-}CSF}$. **B**. Healthy donor PBMC were treated ±VPA for 4 hours followed by $HSV^{GM\text{-}CSF}$ treatment (0.01 and 0.001pfu/cell) overnight. PBMC were co-cultured with melanoma targets and NK cell ($CD56^{+}/CD3^{-}$) CD107 degranulation was determined by flow cytometry. Data shows the mean percentage of NK cells expressing CD107 after co-culture with MEL888 and A375 cell targets (n=3, +SEM).

Supplementary Figure 8

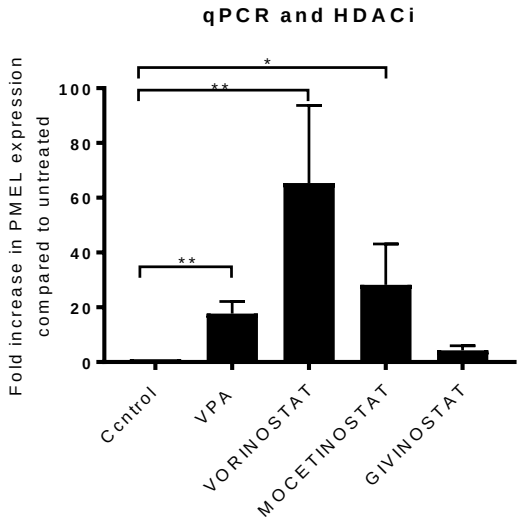

Supplementary Figure 8. Alternative HDACi up-regulate PMEL TAA expression. PMEL mRNA expression levels in A375 cells were quantified by qRT-PCR relative to EF1α housekeeping control following treatment with 2mM VPA (n=6, +SEM), 2µM vorinostat, 1µM mocetinostat and 0.1µM givinostat for 48hrs (n=3, +SEM).